

AD-A098 417

PISA UNIV (ITALY) INST OF AERONAUTICS

F78 1/3

THE FATIGUE CRACK GROWTH UNDER VARIABLE AMPLITUDE LOADING IN RU--ETC (11)

JAN 81 A SALVETTI, G CAVALLINI, L LAZZERI

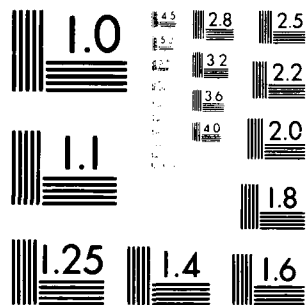
DA-ERG-78-6-107

RL

UNCLASSIFIED

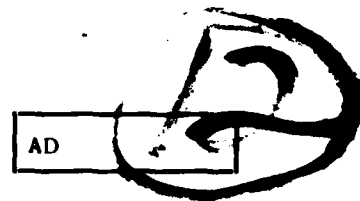


END
DATE
FILMED
5 81
DTIC



MICROCOPY RESOLUTION TEST CHART
NATIONAL BUREAU OF STANDARDS-1963-A

LEVEL II



THE FATIGUE CRACK GROWTH UNDER VARIABLE AMPLITUDE LOADING IN BUILT-UP STRUCTURES

2nd Annual Technical Report

by

A. SALVETTI - Principal Investigator
G. CAVALLINI and L. LAZZERI

January 1981

EUROPEAN RESEARCH OFFICE

United States Army
London England

GRANT NUMBER DA ERO - 78 - G - 107

Istituto di Aeronautica
Università di Pisa
Italy

DTIC
ELECTE
MAY 4 1981
S D D

Approved for public release; distribution unlimited

81 5 01 002

AD A098417

DTIC FILE COPY

AD

THE FATIGUE CRACK GROWTH UNDER VARIABLE AMPLITUDE LOADING IN BUILT-UP STRUCTURES

2nd Annual Technical Report

by

A. SALVETTI - Principal Investigator
G. CAVALLINI and L. LAZZERI

January 1981

EUROPEAN RESEARCH OFFICE

United States Army
London England

Accession For	
NTIS GRA&I	<input checked="checked" type="checkbox"/>
DTIC TAB	<input type="checkbox"/>
Unannounced	<input type="checkbox"/>
Justification	
By	
Distribution/	
Availability Codes	
Dist	Avail and/or Special
A	

GRANT NUMBER DA ERO - 78 - G - 107

Istituto di Aeronautica
Università di Pisa
Italy

DTIC
ELECTE
S MAY 4 1981 D
D

Approved for public release; distribution unlimited

UNCLASSIFIED

SECURITY CLASSIFICATION OF THIS PAGE (When Data Entered)

R&D 2600-AN

REPORT DOCUMENTATION PAGE		READ INSTRUCTIONS BEFORE COMPLETING FORM
1. REPORT NUMBER	2. GOVT ACCESSION NO.	3. RECIPIENT'S CATALOG NUMBER
	AD-A098417	7
4. TITLE (and Subtitle) The Fatigue Crack Growth Under Variable Amplitude Loading in Built-up Structures.		5. TYPE OF REPORT & PERIOD COVERED Annual Technical Report Sept 78 - Oct 80
6. AUTHOR(s) A. Salvetti, G. Cavallini, L. Lazzeri		7. PERFORMING ORG. REPORT NUMBER
8. PERFORMING ORGANIZATION NAME AND ADDRESS Istituto di Aeronautica Universita di Pisa Italy		9. CONTRACT OR GRANT NUMBER(s) DA-ERO-78-G-107
10. CONTROLLING OFFICE NAME AND ADDRESS USARDSG-UK Box 65, FPO NY 09510		11. PROGRAM ELEMENT, PROJECT, TASK AREA & WORK UNIT NUMBERS 6.11.02A 1T161102BH57-06
12. MONITORING AGENCY NAME & ADDRESS (if different from Controlling Office)		13. REPORT DATE January 1981
		14. NUMBER OF PAGES 72
		15. SECURITY CLASS. (of this report) Unclassified
		16. DECLASSIFICATION/DOWNGRADING SCHEDULE
17. DISTRIBUTION STATEMENT (of this Report) Approved for Public Release; distribution unlimited		
18. DISTRIBUTION STATEMENT (of the abstract entered in Block 20, if different from Report)		
19. SUPPLEMENTARY NOTES		
20. KEY WORDS (Continue on reverse side if necessary and identify by block number) Fatigue of built-up structures Metal fatigue Realistic load programs		
21. ABSTRACT (Continue on reverse side if necessary and identify by block number) Research aimed at developing reliable methods for predicting the growth of a crack in built-up aircraft structures under realistic load conditions is currently being carried out at the Institute of Aeronautics of the University of Pisa under a three-year research contract DA-ERO-78-G-107. This paper presents the results obtained in the course of the second year during which, altogether, 33 specimens were tested both at constant and variable Contd...		

DD FORM 1 JAN 73 1473

EDITION OF 1 NOV 65 IS OBSOLETE

UNCLASSIFIED

SECURITY CLASSIFICATION OF THIS PAGE (When Data Entered)

401046

UNCLASSIFIED

SECURITY CLASSIFICATION OF THIS PAGE(When Data Entered)

20. Contd.

amplitude loading. The specimens, cut from sheets of 7075-T6 aluminium alloy, coming from the same batch were both simple sheets and riveted stiffened panels.

The constant amplitude tests on simple sheet specimens were carried out in order to obtain the average K-rate relationship and the relevant scatter of the batch of sheets. The constant amplitude tests on stiffened panel were aimed at obtaining information on rivet flexibility and friction forces.

Variable amplitude tests were performed utilizing the FALSTAFF spectrum. The data on sheet specimens was used to assess the reliability of prediction methods such as those devised by Wheeler and Willenborg, and the stiffened panels test data to establish how these methods work in the case of built-up structures.

The results presented in this paper, especially those concerning the spectrum tests on stiffened panels, are still preliminary, but significant in as far as they allow us to assess the reliability of crack grow prediction methods and to obtain a qualitative but deep insight into the phenomenon of crack growth in built-up structures.

The program of further tests, planned for the third year, has been drawn up with a view to the quantitative assessment of the complex phenomenon described above.

UNCLASSIFIED

SECURITY CLASSIFICATION OF THIS PAGE(When Data Entered)

SUMMARY

Research aimed at developing reliable methods for predicting the growth of a crack in built-up aircraft structures under realistic load conditions is currently being carried out at the Institute of Aeronautics of the University of Pisa under a three-year research contract DA ERO-78-G-107.

This paper presents the results obtained in the course of the second year during which, altogether, 33 specimens were tested both at constant and variable amplitude loading. The specimens, cut from sheets of 7075-T6 aluminium alloy, coming from the same batch, were both simple sheets and riveted stiffened panels.

The constant amplitude tests on simple sheet specimens were carried out in order to obtain the average K-rate relationship and the relevant scatter of the batch of sheets. The constant amplitude tests on stiffened panel were aimed at obtaining information on rivet flexibility and friction forces.

Variable amplitude tests were performed utilizing the FALSTAFF spectrum. The data on sheet specimens was used to assess the reliability of prediction methods such as those devised by Wheeler and Willenborg, and the stiffened panels test data to establish how these methods work in the case of built-up structures.

The results presented in this paper, especially those concerning the spectrum tests on stiffened panels, are still preliminary, but significant in as far as they allow us to assess the reliability of crack growth prediction methods and to obtain a qualitative but deep insight into the phenomenon of crack growth in built-up structures.

The program of further tests, planned for the third year, has been drawn up with a view to the quantitative assessment of the complex phenomenon described above.

TABLE OF CONTENTS

SUMMARY	Page	III
LIST OF ILLUSTRATIONS	"	V
LIST OF TABLES	"	VIII
LIST OF SYMBOLS	"	IX
1 - INTRODUCTION	"	1
2 - TEST PROGRAM AND OBJECTIVES	"	4
3 - TEST PROCEDURE AND DATA EVALUATION	"	6
4 - ANALYSIS OF RESULTS	"	8
4.1 - SIMPLE SHEET-CONSTANT AMPLITUDE TESTS ..	"	8
4.2 - SIMPLE SHEET-VARIABLE AMPLITUDE TESTS ..	"	9
4.3 - CONSTANT AMPLITUDE-STIFFENED PANEL TESTS	"	11
4.4 - VARIABLE AMPLITUDE-STIFFENED PANEL TESTS	"	13
5 - CONCLUSIONS AND FUTURE RESEARCH WORK	"	15
REFERENCES	"	18
APPENDIX 1	"	19
APPENDIX 2	"	20
FIGURES	"	21
TABLES	"	52

LIST OF ILLUSTRATIONS

Figures

Fig. 1 - Regression analysis on all the experimental data for evaluating Forman's law	Page 21
Fig. 2 - Regression analysis on all the experimental data for evaluating Paris-Walker law	" 22
Fig. 3a - Regression analysis on experimental data of group 'A' for evaluating Forman's law	" 23
Fig. 3b - Regression analysis on experimental data of group 'B' for evaluating Forman's law	" 24
Fig. 4a - Regression analysis on experimental data of group 'A' for evaluating Paris-Walker law	" 25
Fig. 4b - Regression analysis on experimental data of group 'B' for evaluating Paris-Walker law	" 26
Fig. 5a - Lognormal cumulative distributions of the variable $N_{ex}/N_{c,A}$ for the constant amplitude tests of group 'A' for two ranges of damage growth	" 27
Fig. 5b - Lognormal cumulative distributions of the variable $N_{ex}/N_{c,B}$ of group 'B' for two ranges of damage growth	" 28
Fig. 5c - Lognormal cumulative distributions of the variable N_{ex}/N_c for two ranges of damage growth	" 29
Fig. 5d - Lognormal cumulative distributions of the variable N_{ex}/N_c for two ranges of damage growth	" 30
Fig. 6a - Experimental results of flat panels tests under FALSTAFF spectrum loading with $S_{max}=24.Kg/mm^2$	" 31
Fig. 6b - Experimental results of flat panels tests under FALSTAFF spectrum loading with $S_{max}=20.Kg/mm^2$	" 32

Fig. 7 - Comparison of experimental results with predictions obtained with the two sets of Forman law constants for flat panels tests under FALSTAFF spectrum with $S_{max}=20.Kg/mm^2$	Page 33
Fig. 7a - Comparison of experimental results with predictions obtained with the two sets of Forman law constants for flat panels tests under FALSTAFF spectrum with $S_{max}=24.Kg/mm^2$	" 34
Fig. 8a - Lognormal cumulative distributions of the variable F_{ex}/F_c for flat panels tests under FALSTAFF spectrum with $S_{max}=20.Kg/mm^2$	" 35
Fig. 8b - Lognormal cumulative distributions of the variable F_{ex}/F_c for flat panels tests under FALSTAFF spectrum with $S_{max}=24.Kg/mm^2$	" 36
Fig. 8c - Lognormal cumulative distributions of the variable F_{ex}/F_c for flat panels tests under FALSTAFF spectra with $S_{max}=20.Kg/mm^2$ and $S_{max}=24.Kg/mm^2$	" 37
Fig. 9 - F_{DATA} versus flexibility parameter ξ for the constant amplitude-stiffened panels tests	" 38
Fig.10a - F_{DATA} versus flexibility parameter ξ for the constant amplitude-stiffened panels tests, taking into account friction forces through the parameter η	" 39
Fig.10b - Continued	" 40
Fig.10c - Continued	" 41
Fig.11a - Regression analysis of the experimental data from constant amplitude tests of the stiffened panels	" 42
Fig.11b - Regression analysis of the experimental data from constant amplitude tests of the stiffened panels	" 43
Fig.12 - Lognormal cumulative distribution of the variable $\Delta N_{ex}/\Delta N_c$ for test LRIC-3	" 44
Fig.13 - Lognormal cumulative distribution of the variable N_{ex}/N_c for tets LRIC-3	" 45

- VII -

Fig.14	- Comparison of the experimental data of the constant amplitude-stiffened panels tests with the prediction obtained using Forman law of group 'A' and ΔK evaluated using different values of ξ , rivet flexibility parameter	Page	46
Fig.15	- Experimental results of the variable amplitude tests of the stiffened panels .	"	47
Fig.16	- Lognormal cumulative distributions of the variable F_{ex} for the variable amplitude tests of the stiffened panels for four ranges of damage growth	"	48
Fig.17	- Comparison of the experimental data of the variable amplitude-stiffened panels tests with the predictions obtained using Forman law of the stiffened panels	"	49
Fig.18	- Schematic representation of a rivet-hole system behaviour	"	50
Fig.19	- Comparison of the experimental data of the variable amplitude-stiffened panels tests with the predictions	"	51

LIST OF TABLES

Tables

Tab.1a	- Main characteristics of the constant amplitude-flat panels tests	Page	52
Tab.1b	- Main characteristics of the variable amplitude-flat panels tests	"	53
Tab.1c	- Main characteristics of the constant amplitude-stiffened panels tests	"	54
Tab.1d	- Main characteristics of the variable amplitude-stiffened panels tests	"	55
Tab.2a	- Dimensions of the specimens used for evaluating the yield stress and tensile strength	"	56
Tab.2b	- Dimensions of the specimens used for K_C evaluation	"	56
Tab.3	- Results of constant amplitude-flat specimens tests	"	57
Tab.4	- Results of the variable amplitude-flat panels tests	"	62
Tab.5	- Results of the constant amplitude-stiffened panels tests	"	66
Tab.6	- Results of the variable amplitude-stiffened panels tests	"	69
Tab.A.1	- Certain mechanical properties of a few flat panels utilized in the tests	"	71
Tab.A.2	- Program of tests for the third year's research	"	72

LIST OF SYMBOLS

a	- Half-crack length, mm
da/dn	- Crack growth rate, mm/cycle
F _{DATA}	- Statistical parameter of regression
K	- Stress intensity factor, Kg/mm ^{3/2}
K _c	- Critical stress intensity factor, Kg/mm ^{3/2}
n	- Number of load cycles
P	- Rivet load, Kg.
R	- Stress ratio
S _y	- Yielding stress, Kg/mm ²
η	- Friction parameter
Δ	- Rivet deflection, mm
ΔK	- Stress intensity factor range, Kg/mm ^{3/2}
ξ	- Flexibility parameter

1 - INTRODUCTION

This paper presents the second year's results of an investigation carried out at the Institute of Aeronautics, Pisa University, under contract DA ERO-78-G-107.

The objective of this investigation is the development of a reliable procedure for evaluating the growth of a crack in a built-up structure under loading conditions representative of the operational environment.

The need for investigation into crack growth in riveted built-up structures under variable amplitude loading springs from two main causes, namely the uncertainty surrounding the computational methods of the stress intensity factor and the complexity of the crack growth interaction effects caused by load amplitude variations.

The difficulty of obtaining accurate values of the stress intensity factor must be ascribed mainly to the uncertainty surrounding the idealization of the forces acting between the stringers and the sheet cover.

As far as the second cause is concerned, certain important prediction methods which take interaction effects into account in evaluating crack growth per cycle, are currently available.

All these methods are essentially empiric and derive their experimental substantiation mainly from tests performed on sheet specimens. Therefore, to increase confidence in these methods it is necessary to resort to data drawn from tests performed on specimens representative of airplane structures under realistic loading conditions.

As a consequence of the above, the possibility of reaching the objective already mentioned i.e. of developing reliable crack growth prediction methods, depends on the solution of the two following problems:

- the development of a reliable method to assess the junction forces in a given built-up structure, and
- the evaluation of the accuracy of the existing methods for predicting crack growth under variable amplitude loading on the basis of test data drawn from built-up specimens.

During the first year's research, great emphasis was laid on the problem of describing the junction forces by means of such quantities as fastener flexibility and the friction forces between the stiffener and the sheet faying surfaces.

At the same time, a systematic effort was made to evaluate the reliability of existing prediction methods for crack growth under variable amplitude loading as a preliminary and essential step towards reaching the main objective.

In particular the results presented in the first Annual Report, /1/, concern the following principal topics:

- development and implementation of a rationale for obtaining information on fastener flexibility and friction forces from constant amplitude crack growth data in stiffened panels
- data on rivet flexibility and friction forces
- development and implementation of a rationale for evaluating the reliability of existing prediction methods (Willenborg, Wheeler, Bell-Eidinoff) with regard to crack growth under variable amplitude loading
- data on the reliability of such methods.

In the second year we turned our attention to the problem of crack growth under variable amplitude loading in built-up structures.

To this end we performed a set of crack propagation tests both at constant and variable amplitudes utilizing both simple sheets and stiffened panels as specimens.

These specimens were made of 7075-T6 aluminum alloy drawn from the same stock of sheets. The standardized load sequence FALSTAFF was used for variable amplitude tests.

All the data from the simple sheet tests, as well as the data from constant amplitude tests in stiffened panels, was treated with the methods previously developed and already outlined in Ref.1.

All these tests are ancillary with respect to the variable amplitude tests in stiffened panels which are directly related to the main objective of the investigation.

They are, nevertheless, strictly necessary since their results in terms of average crack growth data, rivet flexibility and the "best" interactive prediction method are fundamental if we are to obtain a meaningful evaluation of crack growth in stiffened panel to compare with the test data.

At the same time, these tests are important in themselves as they make a useful contribution to knowledge on the problem of crack propagation in aircraft structures.

As far as the variable amplitude tests in stiffened panels are concerned, only a limited number of results have been obtained during the present year.

Such results are nevertheless meaningful as they enable us to successfully check a methodology for interpreting test data, to obtain a significant initial insight into the phenomenon and to acquire the basis necessary for drawing up a conclusive third year's research program.

The main results obtained during this research will be outlined in the following sections.

2 - TEST PROGRAM AND OBJECTIVES

To reach the objectives of the second year's research program a rational sequence of tests was devised.

Two types of specimens were selected, namely simple sheets and riveted stiffened panels. Both types of specimens were prepared utilizing the aluminum alloy 7075-T6 cut from the same stock of sheets. Certain of these specimens were tested at constant amplitude loading, the others at variable amplitude loading on the basis of the FALSTAFF sequence.

Tabs 1a to 1d show the geometric shape and dimensions of the specimens together with initial crack lengths and the relevant load conditions.

The tables give the maximum stress and the stress ratio for constant amplitude tests; in the case of variable amplitude loading, the maximum stress in the spectrum is given.

All the stiffened panels were fastened with countersunk head rivets. The rivets were handriveted by a skilled operator in such a way that the driven head had a diameter approximately equal to $1.4 \div 1.5$ the shank diameter.

Altogether 33 specimens were tested, of which 18 under variable amplitude loading.

The test program was completed by static tests to obtain the σ - ϵ relationship and the K_C with a view to a better characterization of the material used to construct the specimens.

The specimens for this last type of test, whose dimensions are shown in Tabs 2a and 2b, were cut from the specimens utilized for the crack propagation tests after the completion of the tests.

These different types of tests were devised to obtain all the significant information necessary to interpret the data obtained by testing stiffened panels under the FALSTAFF se-

quence.

In particular, the constant amplitude loading test on simple sheets were devised to obtain average crack growth data and the relevant scatter for the material, namely sheets of 7075-T6 aluminum alloys with 1.27 mm of thickness.

The spectrum loading tests on simple sheets were planned to obtain a comparison between different methods suitable for predicting the crack growth under variable amplitude loading.

The methods considered in the present investigation are those already assessed in the course of the first year's activity, /1/, namely

- non interactive
- Willenborg and
- Wheeler for different values of the plastic zone constant.

The purpose of the comparison is to select a sufficiently accurate method to be used in the evaluation of crack growth data in stiffened panels under spectrum loading.

The constant amplitude tests on stiffened panels was devised to obtain a quantitative assessment of fastener flexibility and friction forces, together with the "best" average ΔK -rate relationship and the relevant scatter. Such test data is also useful for assessing the actual influence of the friction forces on crack growth and to evaluate the accuracy of simplified prediction methods which allow for the friction forces only by means of an equivalent fastener flexibility.

The results of all tests previously outlined, besides being significant in themselves, give us the necessary background for adequately interpreting the crack growth data obtained from variable amplitude tests on stiffened panels. This last type of test, which is the most significant as far as

the objectives of the present investigation are concerned, was carried out only to limited extent in the course of this second year's activity.

These tests were mainly planned in order to obtain an initial but nevertheless penetrating insight into the complex phenomenon of crack growth in built-up structures, to check the accuracy of the prediction method we had developed and to create the background for a rational planning of the third year's test activity.

3 - TEST PROCEDURE AND DATA EVALUATION

All the specimens were tested in a load apparatus, already described in /1/, which essentially is composed of a rig, plates for specimen clamping, a servocontrolled hydraulic actuator, capable of ± 250 KN and fed by an electrical signal which in spectrum tests is generated by a PDP 11/34 computer, and an optical device to read the crack length with an accuracy of 0.1 mm.

All the test data was recorded in the form of the crack length versus the number of cycles or the number of flights, whichever was appropriate.

All this data was then treated following the methodologies presented in Ref.1.

In particular, the a-n data of the sheet specimens was processed utilizing the SKESA computer program on the basis of the rationale given in Fig. 12 of Ref.1, in order to obtain the constants which define the semi-empirical laws of crack propagation (Paris-Walker and Forman, typically) and the scatter in crack length prediction.

The data from sheet-specimens tested under the FALSTAFF spectrum was treated, utilizing initially the CADAV computer program, Ref.1, which computes the numbers of flights neces-

sary to reach a given crack length on the basis of the following methods: non-interactive, Willenborg method and Wheeler for different values of the plastic zone parameter, m .

The predictions of the different methods are then compared on a statistical basis, Ref.1, with the test data in order to find the best method, namely the one which agrees on average with the experimental results in terms of a versus N or a versus F .

The experimental data a - n derived from testing stiffened panels under constant amplitude loading are processed to obtain the following results

- rivet flexibility
- friction forces
- da/dn versus ΔK .

As far as the first two quantities are concerned, the optimization procedure outlined in Ref.1, based on the SKESA computer programme, which fits the test data with a Paris or Forman law, is carried out. The values of flexibility and friction are systematically varied and their best values are selected as those which minimize the standard deviation between the test data and each best fit relevant to the different couples of values of flexibility and friction force.

Once the best values have been determined, the da/dn versus ΔK is then obtained.

Lastly, the variable amplitude loading test data relevant to the stiffened panels is processed on the basis of the following procedure:

- computation of the stress intensity factor utilizing the best values of the flexibility and friction forces as deduced from constant amplitude tests
- computation of cycle by cycle growth due to a FALSTAFF load sequence utilizing the Wheeler method with appropriate value of the plastic zone constant, deduced from sheet tests. This computation is carried out utilizing the da/dn -

ΔK relationship relevant to the stiffened panels since it was found to be different from the one obtained with simple sheet

- comparison of computed and experimental data.

4 - ANALYSIS OF RESULTS

All the experimental results are given in tabs 3,4,5, and 6, in terms of $a-N$ or $a-F$ in relation to the type of test carried out.

All this data has been treated on the basis of the procedures outlined in the previous section.

The main results of this treatment will be presented in the following sections.

4.1 - SIMPLE SHEET-CONSTANT AMPLITUDE TESTS

The data in Tab. 3 was processed in order to obtain the usual ΔK -rate relationship.

Fig.1 presents such a relationship in the form of Forman's law, whereas Fig. 2 is relevant to the Paris-Walker law. Irrespective of what kind a law is used, the data is likely to belong to two different scatter bands, one being the A band characterized by a higher rate, the other, the B band, characterized by a lower rate.

Because of these different sorts behaviour, it was decided to evaluate the constants of the propagation laws separately for each scatter band. These results are shown in Fig. 3a, and 3b for the Forman law and in Fig. 4a and 4b for the Paris-Walker law.

Because of these results it was decided to check the static strength and the toughness of the material used for the specimens tested. To this end the specimens in Tab. 2 have been tested, producing the results given in Appendix 1.

These tests show that the material has fairly uniform characteristics in terms of σ_y , σ_R and K_C so that the two kinds of behaviour cannot be explained on the basis of different material static characteristics.

So at present no rational explanation of the phenomenon can be formulated even if all the data in Fig. 1 falls well within the typical scatter band reported in the literature, /2/, for this material.

Fig. 5a and 5b are relevant to the scatter of crack growth predictions, in terms of the number of cycles necessary to reach a given crack length.

$N_{C,A}$ is the number of cycles computed with the best fit of the A band, and $N_{C,B}$ the same quantity relevant the B band, N_{ex} is the experimental data. Fig. 5c shows the same type of probability plot where N_C is calculated or with A or with B best fit, whichever is appropriate.

This last plot shows that $Lg \frac{N_{ex}}{N_C}$ conforms to normal low-scatter distribution when N_C is computed with the appropriate scatter band best-fit.

Lastly, Fig. 5d shows the scatter of the prediction when all the data in Fig.1 is considered to belong to the same population.

The comparison of Fig.5c and 5d shows how the scatter of prediction can be affected by the constants selected for the propagation law.

4.2 - SIMPLE SHEET-VARIABLE AMPLITUDE TESTS

Variable amplitude loading tests were carried out by applying a FALSTAFF spectrum to sheet specimens equal to those used in constant amplitude tests Tab. 4. Two groups of tests have been performed; the first group, which comprises six specimens, is characterized by a maximum stress

in the spectrum of 24 Kg/mm²; the second group, also of six specimens, by a maximum stress equal to 20 Kg/mm².

Plots of a versus F are shown in figs 6a and 6b.

The different curves in fig. 6a agree fairly well the one with the other.

On the contrary, the data of fig. 6b looks widely scattered.

Closer examination of this last set of data shows that this data can be considered as belonging to two different groups, namely groups A and B already found in simple sheet-constant amplitude data.

To verify this hypothesis, the data relevant to curves 8, 11, 12 was processed with the CADAV computer program utilizing the Forman law with the constants pertaining to scatter band A, whereas the data of curves 7, 9, 10 was processed with the constants of scatter band B.

The results of this analysis, given in Fig. 7 where the experimental results are compared with the prediction data, seem to indicate that such hypothesis may explain the scatter in Fig. 6b.

Fig. 8a is the usual plot of the cumulative probability distribution of the random variable $\text{Log } \frac{F_{ex}}{F_c}$ where F_c was computed, for each of the methods shown, utilizing the constants of the Forman law which are appropriate to the groups (A or B) F_{ex} belongs to.

Fig. 8b gives the same plot for the specimens in Fig. 6a.

The scatter of this data is lower than that in Fig. 8a, but still of the same order as is clearly seen from a comparison of the standard deviations.

Fig. 8c gives the cumulative probability distribution for all the data (20 and 24 Kg/mm²).

The random variable $\text{Log } \frac{F_{ex}}{F_c}$ still conforms to normal distribution with standard deviation higher than, but still

comparable with the values shown in Figs 8a and 8b. The results shown in the last three figures are based on the methods of Willenborg and Wheeler alone. The results relevant to the non-interactive and Bell methods have been deleted. The first always gives too conservative results with this type of spectrum, /1/, whereas the second method was found to be unaccurate due to uncertainty affecting the constants characterizing the effects of interaction in the material used in the present investigation.

4.3 - CONSTANT AMPLITUDE-STIFFENED PANEL TESTS

Five stiffened panels out of eleven were tested at constant amplitude loading to obtain the necessary information on rivet flexibility and friction forces.

Such quantities were evaluated following the procedure discussed in Ref.1 and outlined in section 3.

Fig. 9 shows the flexibility ratio $\xi^{(0)}$ as a function of the Fischer variable obtained regardless of the effect of friction forces.

The best assessment of ξ , namely its most probable value, falls for the different panels within a very small range, and assumes the value $\xi = 0.10$ when all the data is considered to belong to the same population.

This very low scatter in the ξ values may be ascribed to the riveting techniques which guaranteed close tolerance on the diameter of the driven head. On the contrary, the stiffened panels used in the tests reported in Ref. 1 were riveted by different operators without a specification as far as driven head diameter was concerned.

(⁰) ξ is the ratio of the actual flexibility and the flexibility as computed according to Swift's formula given in Ref.1.

This state of affairs must probably be considered the main cause of the larger dispersion in ξ reported in Ref.1.

The next step was the evaluation of the influence of friction. The results are shown in Fig.10 where F_{DATA} is plotted against ξ for different values of η , namely the ratio between the resultant friction force within a rivet spacing, acting halfspacing, and a reference axial force in the rivet corresponding to the yielding stress.

A best value of η very close to 0.15 is found without any significant scatter.

Figs 11 compare the ΔK -rate relationship in the two cases of the best flexibility without friction and the best flexibility with the best friction. The differences between the two best fit lines are very small; so the accuracy of crack length predictions can seldom be impaired if friction forces are disregarded, at least, with the present results.

This statement is supported by the data in Fig. 12 which gives the cumulative probability distribution in the first case.

This result is worth pointing out because of the extreme simplification in the analysis that is obtained disregarding friction.

One puzzling result emerging from a comparison of Fig.1 and Fig. 11 is the significant difference between the best-fit lines in the two cases of the stiffened panels and the simple sheets.

To check that this difference does not stem from the method we devised to evaluate the flexibility and friction forces, we also tackled the problem from another point of view.

The number of cycles necessary to reach a given crack length was computed utilizing the A-type ΔK -rate relationship of sheet specimens, and different values of the flexibility ratio ξ . Then, utilizing the usual probabilistic approach, the curves in Fig.13 were plotted. The best value of ξ was selected, the best being

that which assures $(1-P) \cdot 100 = 50$ corresponding to $\text{Log } \frac{N_{ex}}{N_c} = 0$.

The result obtained in this way, that seems to indicate a high flexible fastener behaviour, is remarkably different from that given by the previous method. In order to obtain deeper knowledge on the question, we compared the experimental data $a-N_{ex}$ with the $a-N_c$ values calculated both by means of the ΔK -rate of the stiffened panels with the relevant best value of ξ , and the A group ΔK -rate with the best value of ξ given in Fig. 13.

This comparison, contained in Fig. 14, clearly shows that the $a-N$ values calculated by means of the stiffened panel ΔK -rate very closely fit the test data in the flex zones too.

The other approach, on the contrary, produces a curve $a-N$ which does not tally with the test data.

Consequently, the discrepancy between the stiffened panel and the sheet ΔK -rate relationships cannot be ascribed to errors in our original computing methods of ξ which, on the contrary, work very well.

At present no rational explanation of this discrepancy can be formulated.

4.4 - VARIABLE AMPLITUDE-STIFFENED PANEL TESTS

Six stiffened panels were tested using the FALSTAFF sequence with a maximum stress equal to 20 Kg/mm^2 .

The results of these tests are shown in Fig. 15 in the usual form of a versus F plots.

The scatter of the data, evaluated by plotting $\text{Lg } F_{ex}$ versus probability, is shown in Fig. 16. The standard deviation is higher than that found in the case of stiffened-panels constant-amplitude tests, but the amount of data is too small to attribute this higher scatter to the existence of two different populations.

Fig. 17 contains a comparison between the test data and the prediction made with the methods devised by Wheeler and Willenborg, utilizing the ΔK -rate relationship of the stiffened panels, a flexibility ratio $\xi=0.10$ and friction force parameter $\eta=0$.

The prediction agrees with the test data only in the range of the small crack lengths, say $a < 30$ mm. For greater lengths, the rate of increase per flight of the crack is much higher for the experimental data than for the calculated values.

An explanation of these two different kinds of behaviour in test and computer results may be the plastic deformation of the rivet-hole system due to the load peaks in the FALSTAFF spectrum.

The computer program we used to calculate the stress intensity factor allows for rivet-hole plastic deformation by means of a two straight lines-load displacement relationships, as shown in Fig. 18a, but does not take into account the fact that rivet unload is initially elastic, Fig. 18b. The computer evaluates ΔK as a difference of two successive computation $K_1 - K_2 = \Delta K$ performed utilizing only the OAB part of the load-displacement relationship.

This method is likely to be incorrect especially for long crack lengths whereas the load peaks in the spectrum are likely to produce significant plastic deformations in certain highly loaded rivet-hole systems. Part c of Fig. 18 contains a schematic representation of the deformation of a rivet-hole system. Sketch c_1 represents the rivet-hole behaviour in the linear part OA of the curve; sketch c_2 the plastic-elastic behaviour in the part ABC of the curve and sketch c_3 the part CO of the curve where clearance exists between the rivet and the hole due to previous plastic deformation of the hole. Therefore, if a sufficiently high load is applied corresponding to

a sufficiently long crack, the rivet load follows the loop OABCO. In these conditions, the rivet becomes completely ineffective at least for all the loads of smaller amplitude which produce displacements of the rivet lower than OC.

While waiting for modifications of the computer program allowing us to take into account the behaviour we have described, we performed a preliminary estimation of the crack growth in the long crack length range by completely disregarding the actions of the first line of rivets immediately adjacent to the crack. The results of this approach are given in Fig. 19 which seems to prove our hypothesis on such a phenomenon is correct.

5 - CONCLUSIONS AND FUTURE RESEARCH WORK

The research carried out during the second year of the programme was centered on tests of sheets and stiffened panels loaded both at constant and variable amplitudes. The results of these tests, processed with the methods developed mainly during the first year's activity, have been presented in previous sections.

As far as the attainment of the main objective of the research is concerned, namely the development of a reliable method for predicting crack growth in built-up structures under variable amplitude loading, our results allow us to make significant progress.

The first result concerns the scatter used in the present investigation, namely the aluminium alloy 7075-T6 in sheets 1.27 mm. thick. Specimens cut from a batch of sheets supplied by the same manufacturer, whose yield, strength and toughness are virtually constant, produced crack growth data (da/dn versus ΔK) lying in two different scatter bands and belonging, it would seem, to two different statistical populations. Within each population the scatter is low, but if we force all the

data to belong to a same population, the reliability of prediction decreases significantly, as can be seen from the comparison in Fig. 5d.

The existence of a potentially high scatter in 7075-T6 is a result which is to be expected.

The crack growth data, collected and analyzed in Ref. /2/, has an average K-rate relationship which is very close to that of the present investigation and the scatter is even higher. However, it is worthwhile pointing out the band behaviour we found.

The variable amplitude load tests were carried out using a FALSTAFF spectrum with two different stress levels. In this case too, we found the two bands behaved in the way already described.

The test data in terms of the number of flights necessary for a crack to grow to a given length compares fairly well with the same figures computed by means of the Wheeler method with an appropriate value of the plastic zone constant, only if we select the K-rate relationship relevant to the band the data belong to. Otherwise, the prediction can be poor as can be argued from the data in Figs 12 and 13, which clearly shows the role played by the basic material constants in the whole process of prediction.

Stiffened panel specimens were tested at constant amplitude loading to obtain information on flexibility and friction forces. The results obtained showed that the two quantities mentioned above tend to assume well defined values when riveting is performed by a skilled operator, guaranteeing that the dimensions of the driven rivet head fall within very restricted limits. In these conditions, it was found that if friction forces are neglected, the prediction is still good if the equivalent rivet flexibility is used. This is an interesting result since allowance for friction forces implies

a noteworthy increase in complexity and in the costs of computation.

Another result of these tests is that the best-fit ΔK -rate relationship of the stiffened panels is different from that pertaining in simple sheets. Whether this difference is to be ascribed to the existence of a third scatter band or to a particular kind of behaviour of this type of specimen is still an open question. Further data is necessary for better insight into this phenomenon.

The variable amplitude tests on stiffened panels showed that accurate predictions of the crack growth in a given number of flights can be obtained by means of the CADAVID computer program using the Wheeler method appropriate to the spectrum together with the K-rate relationship and the flexibility value calculated by means of the stiffened panel constant amplitude tests.

However, such predictions may become greatly unconservative if the crack length is relatively large, probably because of the progressive out-of-roundness of the most loaded rivet-holes caused by the combined action of crack length and load peaks in the spectrum.

As far as future research work is concerned, we shall carry out the test program outlined in Appendix 2.

Simple sheets and stiffened panels will be tested utilizing different types of spectra (FALSTAFF, MINITWIST and Gaussian random) which may be considered to be representative of several areas of aircraft operations. These tests will be carried out following the same methods discussed in the present paper and will be processed with the methods already outlined, with further improvements as far as ΔK evaluation in stiffened panels is concerned.

The aim of this last year's set of tests is to present conclusions on the role that the different ingredients (material constants prediction methods and ΔK evaluation via

flexibility and plasticity modelling) have in the prediction of the number of flights necessary for a crack to grow to a given length. Since the inherent material scatter can significantly mask all the other influences, we decided to utilize only the 2024-T3 aluminium alloy, that, in our experience, tends to behave in a more definite way, at least when the specimens are cut from the same batch of sheets.

Notwithstanding this limitation in material selection, this new test program has been conceived with a view to obtaining results which are sufficiently general as far as their application to built-up structures is concerned.

REFERENCES

- /1/ SALVETTI A., CAVALLINI G., LAZZERI L. - The Fatigue Crack Growth Under Variable Amplitude Loading in Built-Up Structures.
DA-ERO-78-G-107, 1st Annual Technical Report, November 1979, I.C.A.F. Doc. 1139.
- /2/ RICE R.C. et al. - Consolidation of Fatigue and Fatigue-Crack-Propagation Data for Design Use. NASA CR-2586, October 1975.

APPENDIX 1 - TESTS FOR THE EVALUATION OF THE MECHANICAL PROPERTIES OF THE MATERIAL.

Tests were performed to evaluate the possible differences in the mechanical properties of the material used in the crack-propagation tests. To this end, four small samples were cut from the flat specimens used in the crack-propagation tests both under constant amplitude and variable amplitude loading. The first kind of test aimed at evaluating the yield stress and the tensile strength of the material. The samples used in these tests were similarly shaped to ASTM standard specimens, but slightly smaller in size. The second kind of test was performed on rectangular specimens with a central through crack: the load applied was increased until the crack length began to propagate and continued to increase up to final failure. The K_C app. values reported in Tab.A1 can be used only as qualitative measurements to assess if the material toughness is comparatively the same for all the specimens. Besides the reduced width of the small specimens in comparison with the dimension of the usual crack-propagation specimen, the K_C app. values were evaluated using the initial crack half-length and the maximum load applied, under which failure occurred. All the values shown in Tab.A1 are the average values for two small specimens belonging to the same specimen used in the crack-propagation tests.

APPENDIX 2 - THIRD YEAR TEST PROGRAM.

The purpose of this appendix is to outline a tentative test program to be carried out in the third year. Tab.A2 shows tentatively the types of specimens and tests.

The test n° 1 will be carried out to determine the semi empirical laws of the crack propagation rate relevant to the batch of sheets we will use in this last phase of the research. Further tests, with specimens not shown in the table, will be performed to characterize the material in terms of σ - ϵ curves and fracture toughness.

The behaviour of material in relation to spectrum types and spectrum levels will be explored by the tests n° 2-7. The results will be utilized for a further evaluation of the reliability of the crack growth prediction methods in structures where the structural behaviour and the stress intensity factor solutions are well established.

The behaviour of the riveted joint will be examined by the successive tests. Tests n° 8 and 9 will give informations about phenomenon of load transmission between sheet and stiffeners; the simplified structure (strip stiffened panel) will be used and two types of rivets will be investigated.

Further tests, such as standard static tests on riveted joint and stiffness measurement of riveted joint after overload application, will be carried out to obtain a more accurate modelling of the elasto-plastic behaviour of the joint.

The behaviour of riveted stiffened panels under spectrum loading and the capability of crack growth prediction methods for these structures will be analysed by the tests n° 10 to 15.

Finally an application to more realistic structures of the results and methodologies obtained will be made by tests n° 16 and 17.

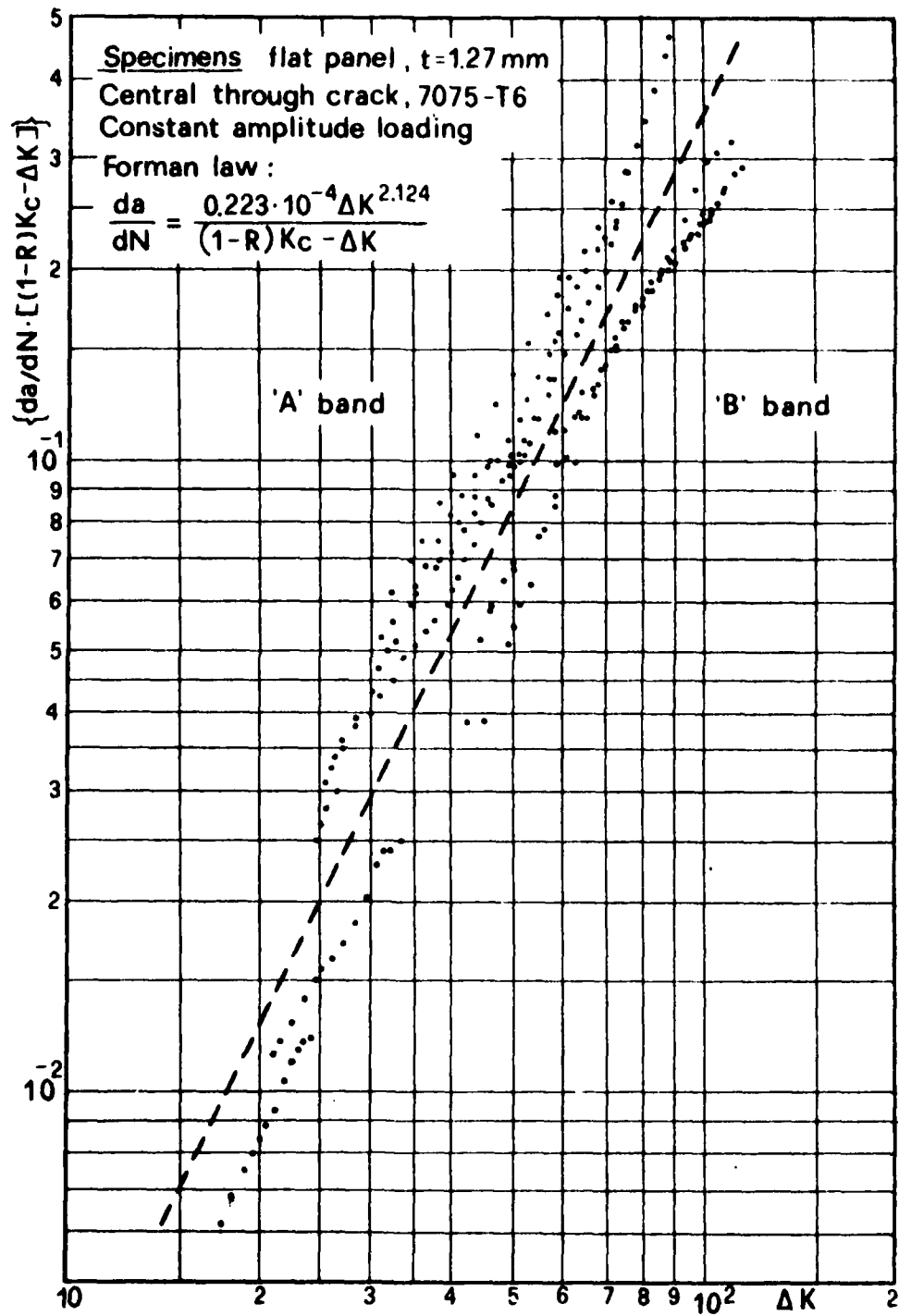


Fig. 1 - Regression analysis on all the experimental data for evaluating Forman's law. The law indicated is the one obtained if the data is supposed to belong to the same population.

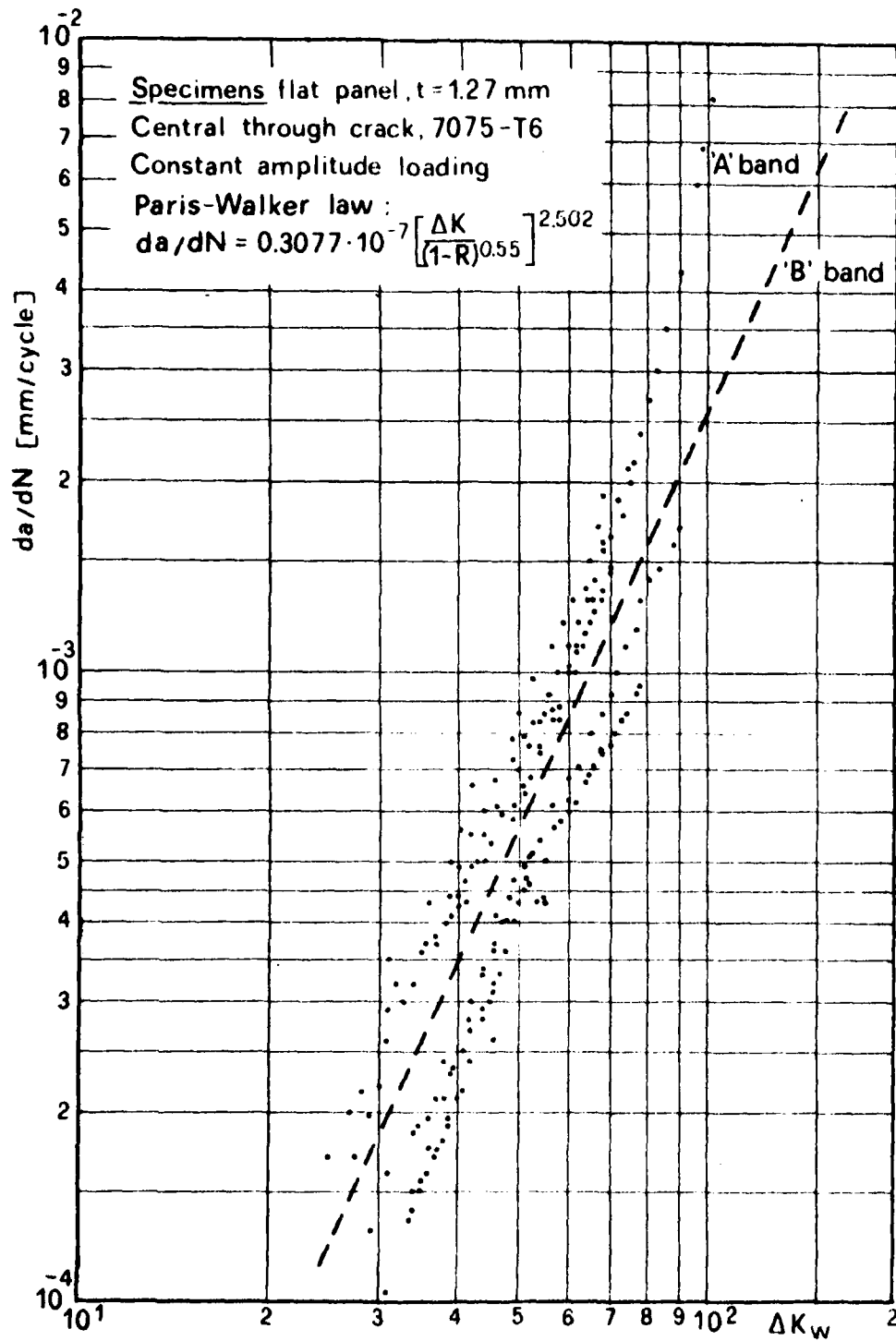


Fig. 2 - Regression analysis on all the experimental data for evaluating Paris-Walker law. The law indicated is the one obtained if the data is supposed to belong to the same population.

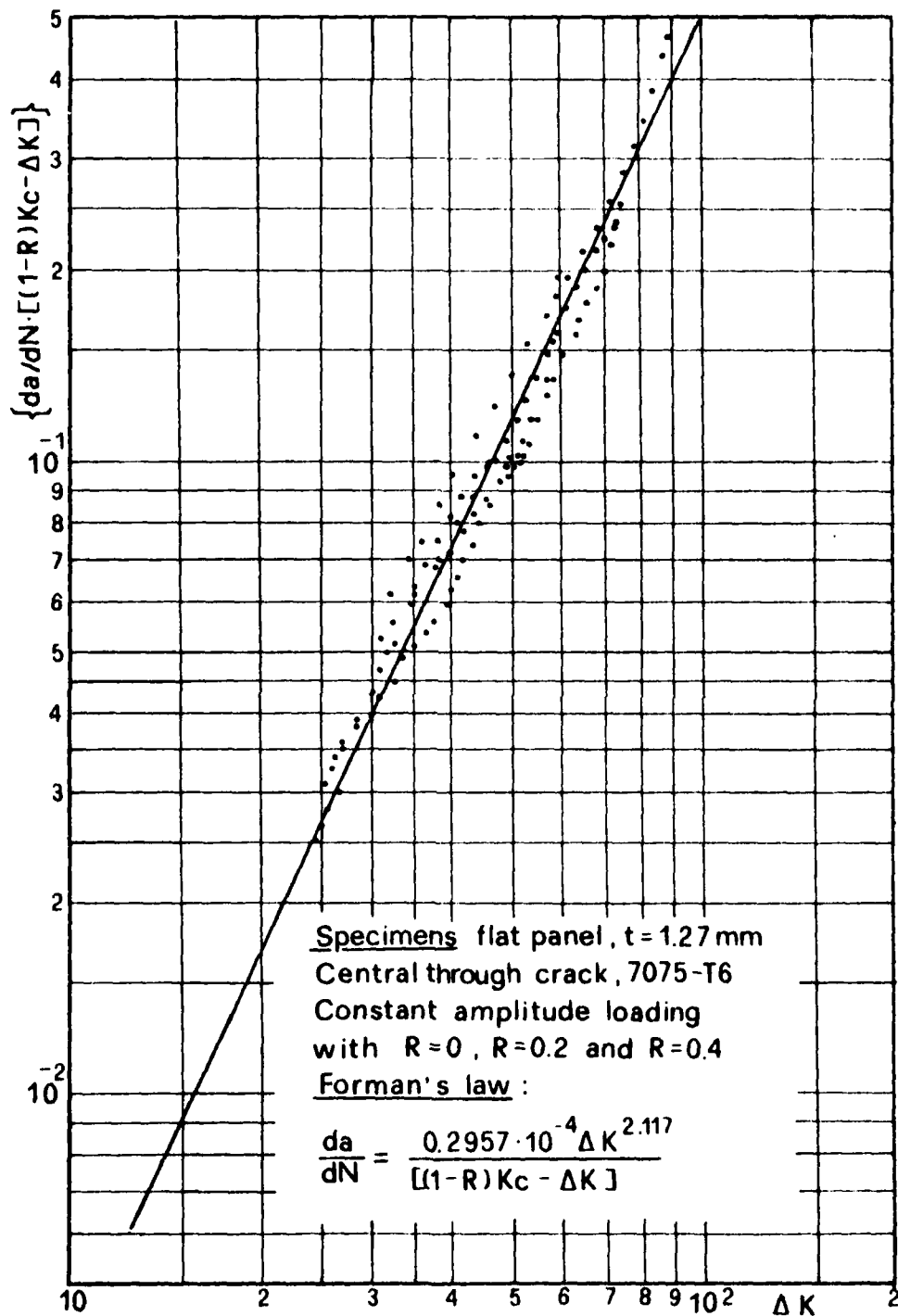


Fig. 3.a - Regression analysis on experimental data of group 'A' for evaluating Forman's law.

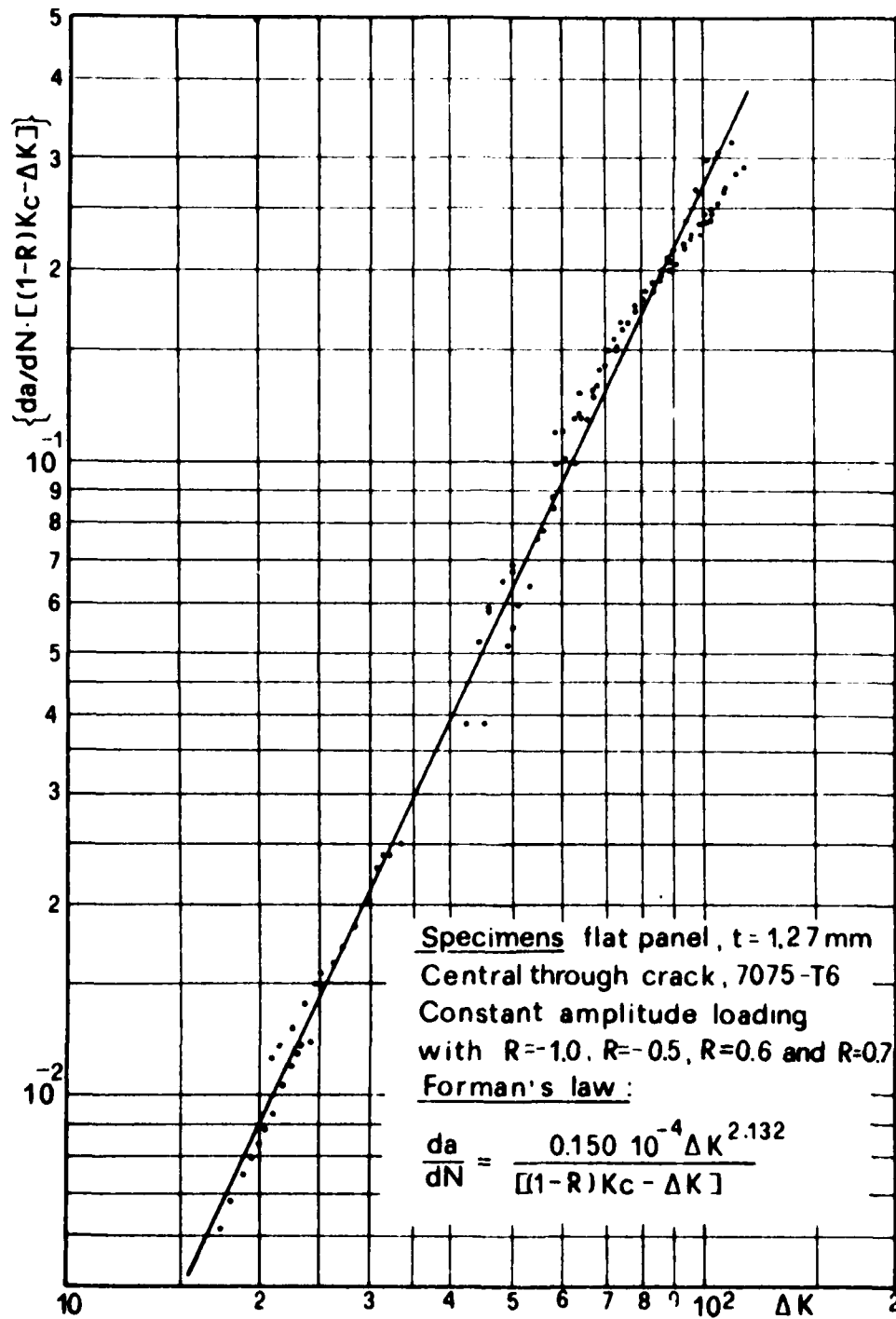


Fig. 3.b - Regression analysis on experimental data of group 'B' for evaluating Forman's law.

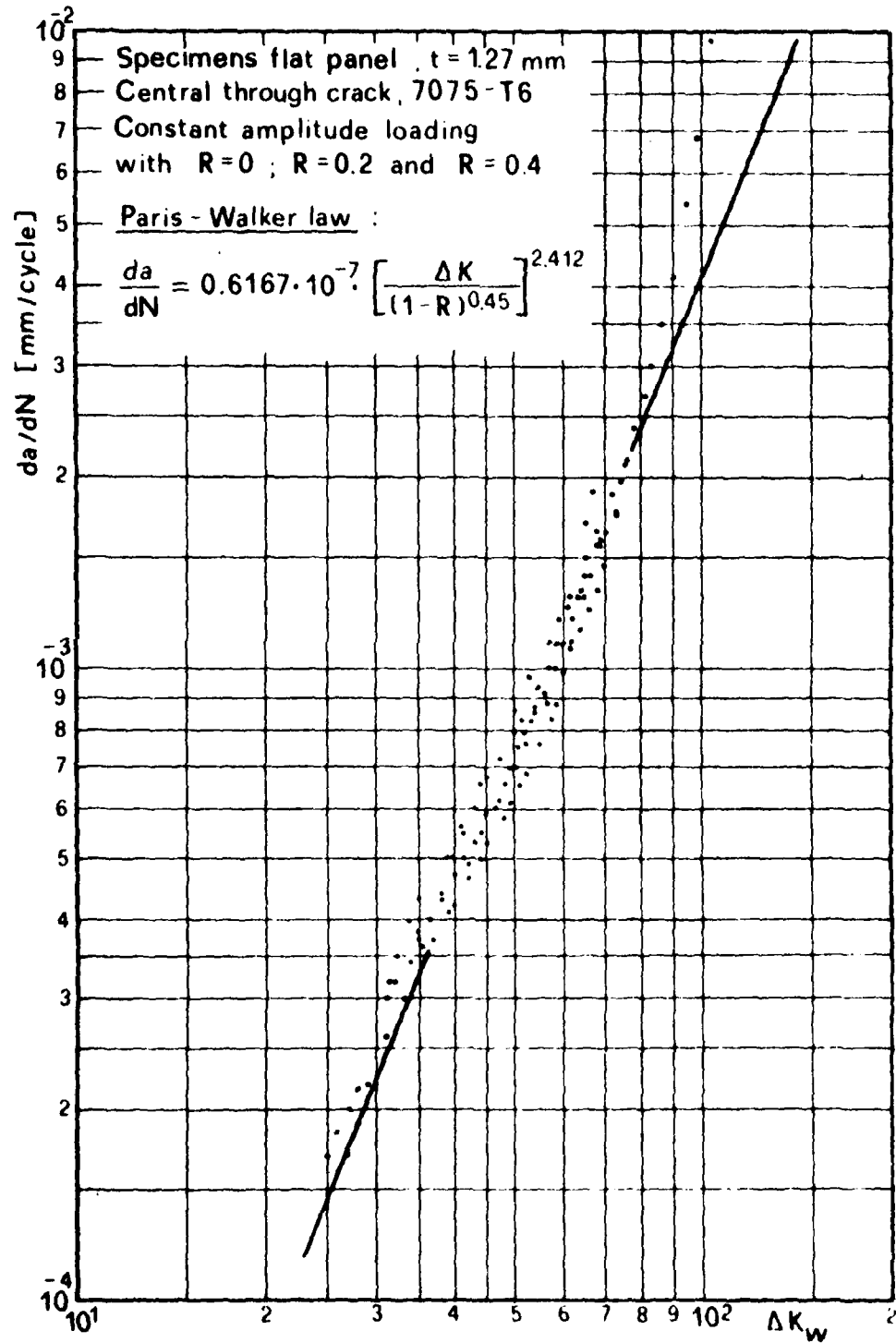


Fig. 4.a - Regression analysis on experimental data of group 'A' for evaluating Paris-Walker law.

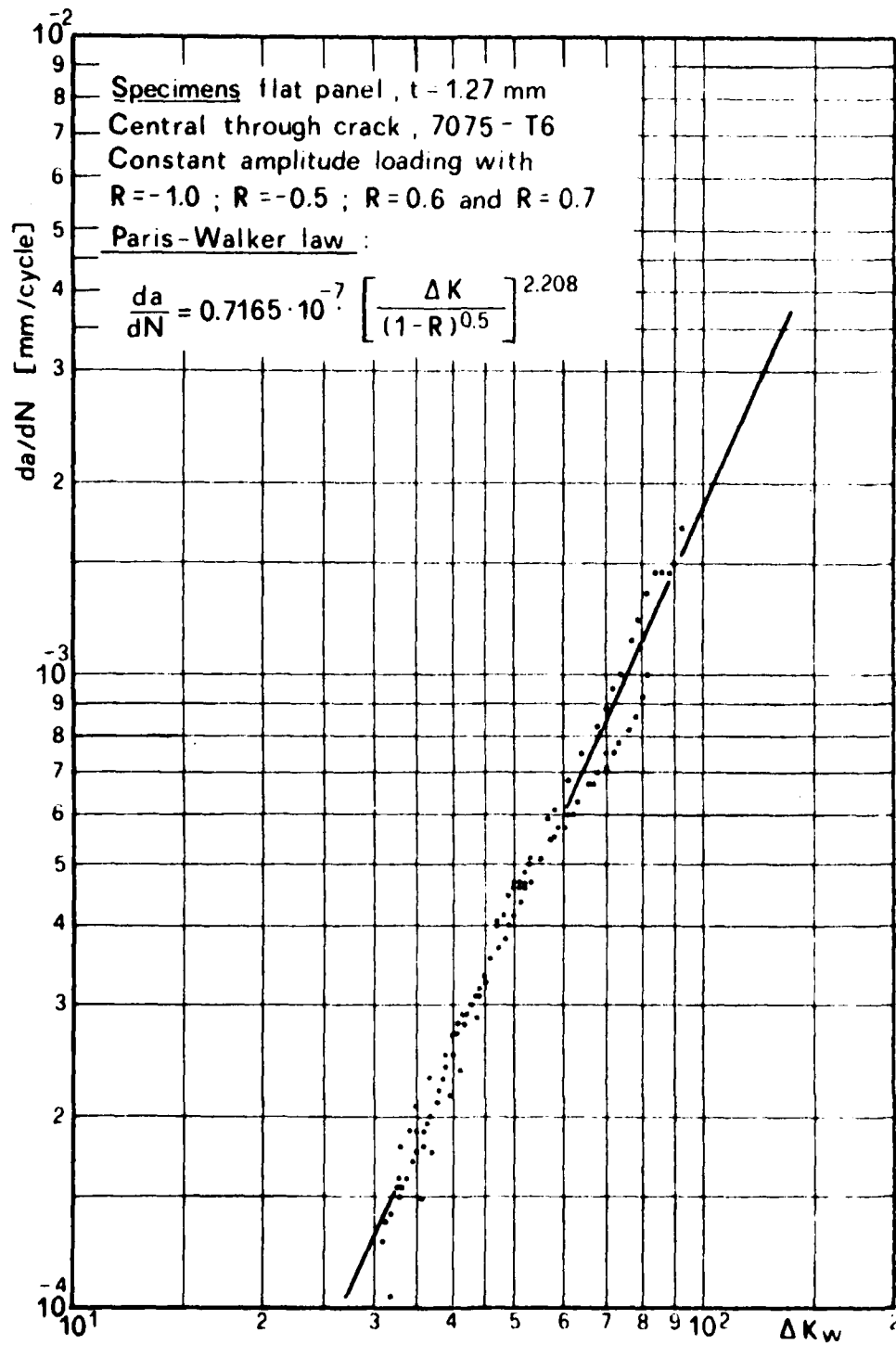


Fig. 4.b - Regression analysis on experimental data of group 'B' for evaluating Paris-Walker law.

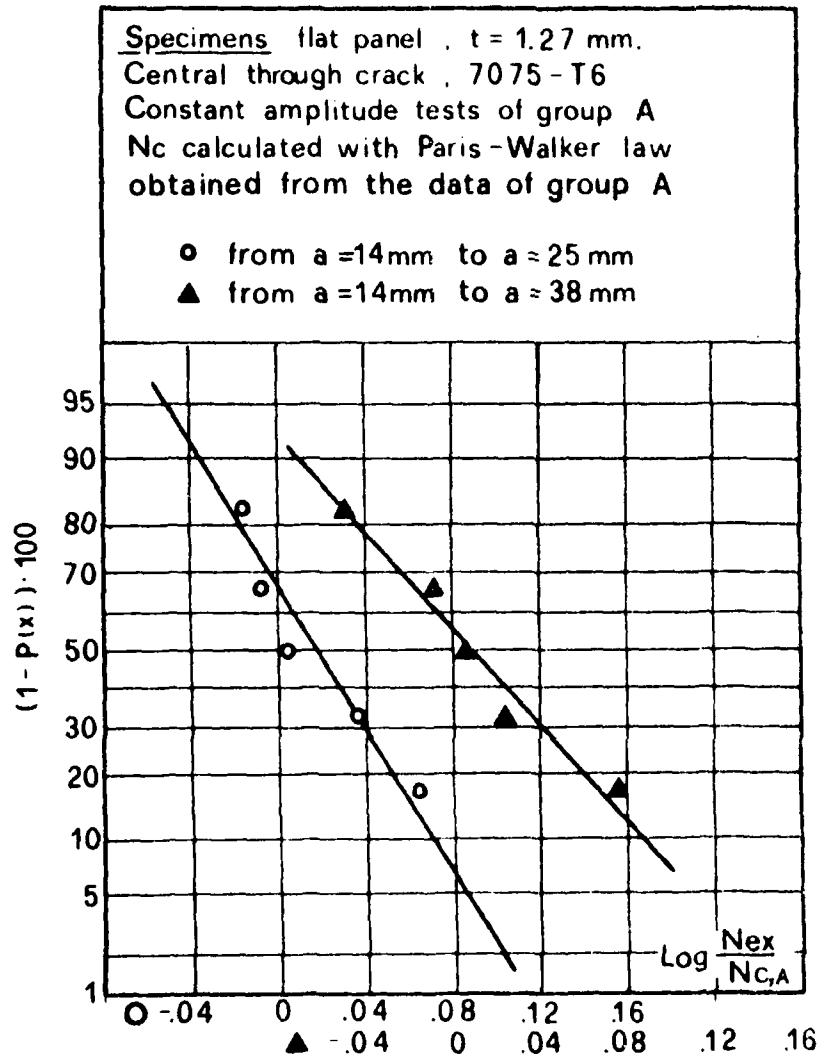


Fig. 5.a - Lognormal cumulative distributions of the variable $N_{ex}/N_{c,A}$ for the constant amplitude tests of group 'A' for two ranges of damage growth.

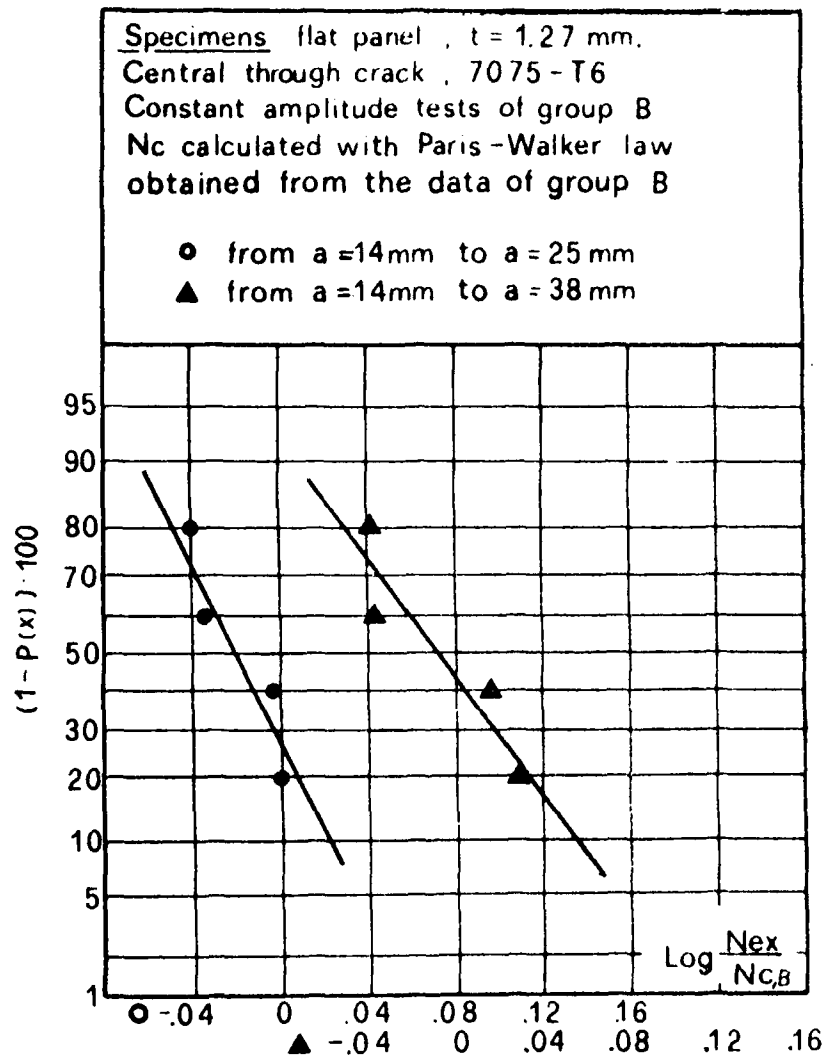


Fig. 5.b - Lognormal cumulative distributions of the variable $N_{ex}/N_{c,B}$ of group 'B' for two ranges of damage growth.

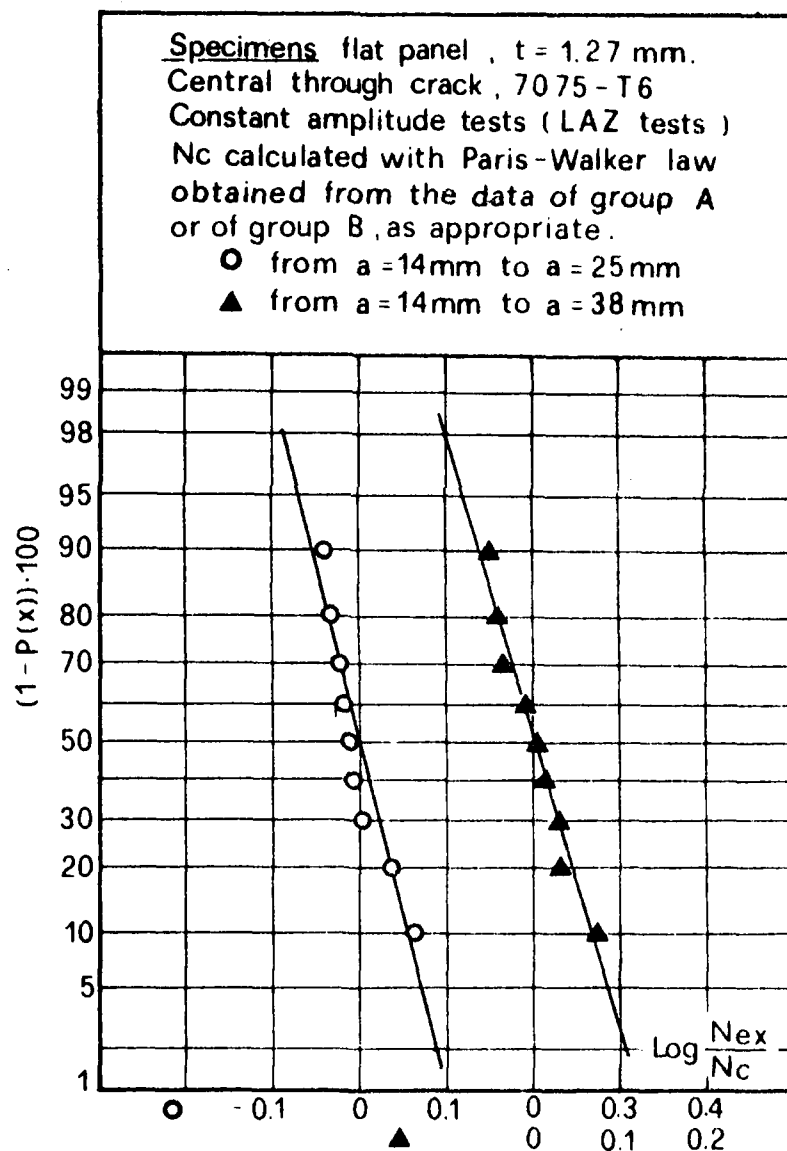


Fig. 5.c - Lognormal cumulative distributions of the variable N_{ex}/N_c for two ranges of damage growth. N_c has been evaluated with Paris-Walker law of growth 'A' or 'B', as appropriate.

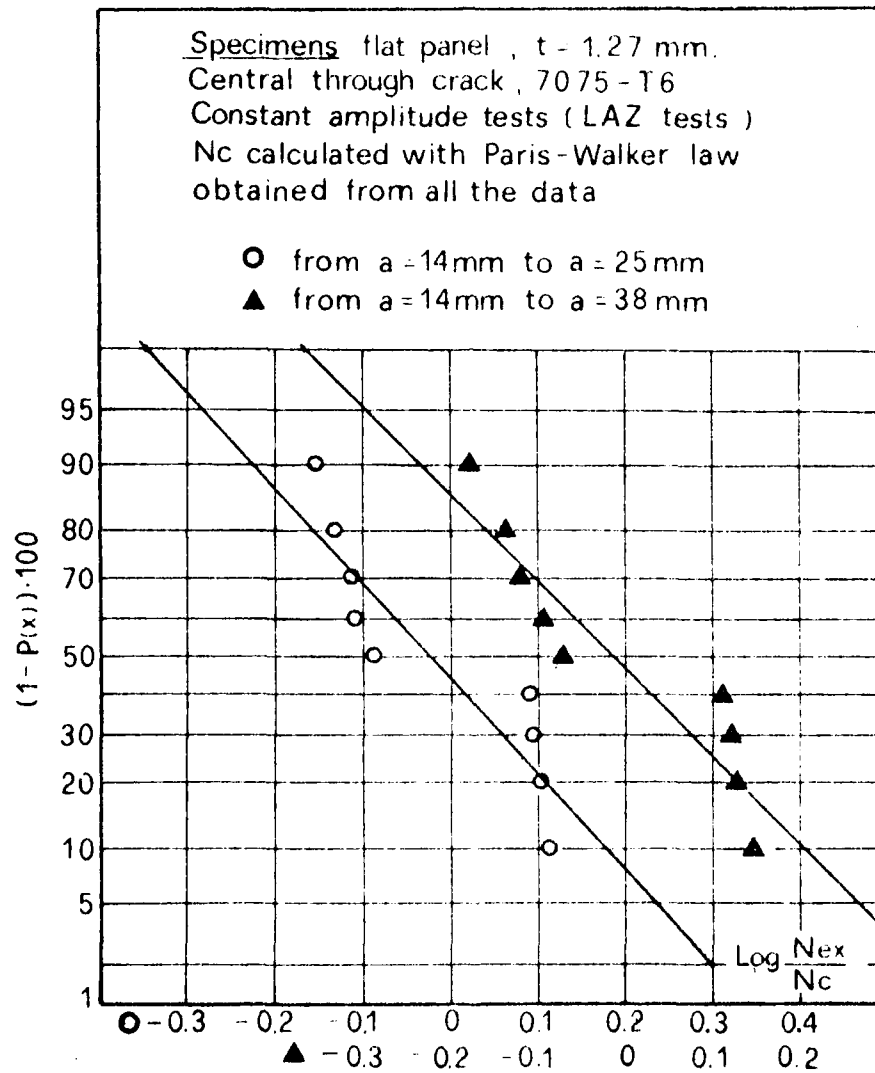


Fig. 5.d - Lognormal cumulative distributions of the variable N_{ex}/N_c for two ranges of damage growth. N_c has been calculated with the Paris-Walker law of Fig.2.

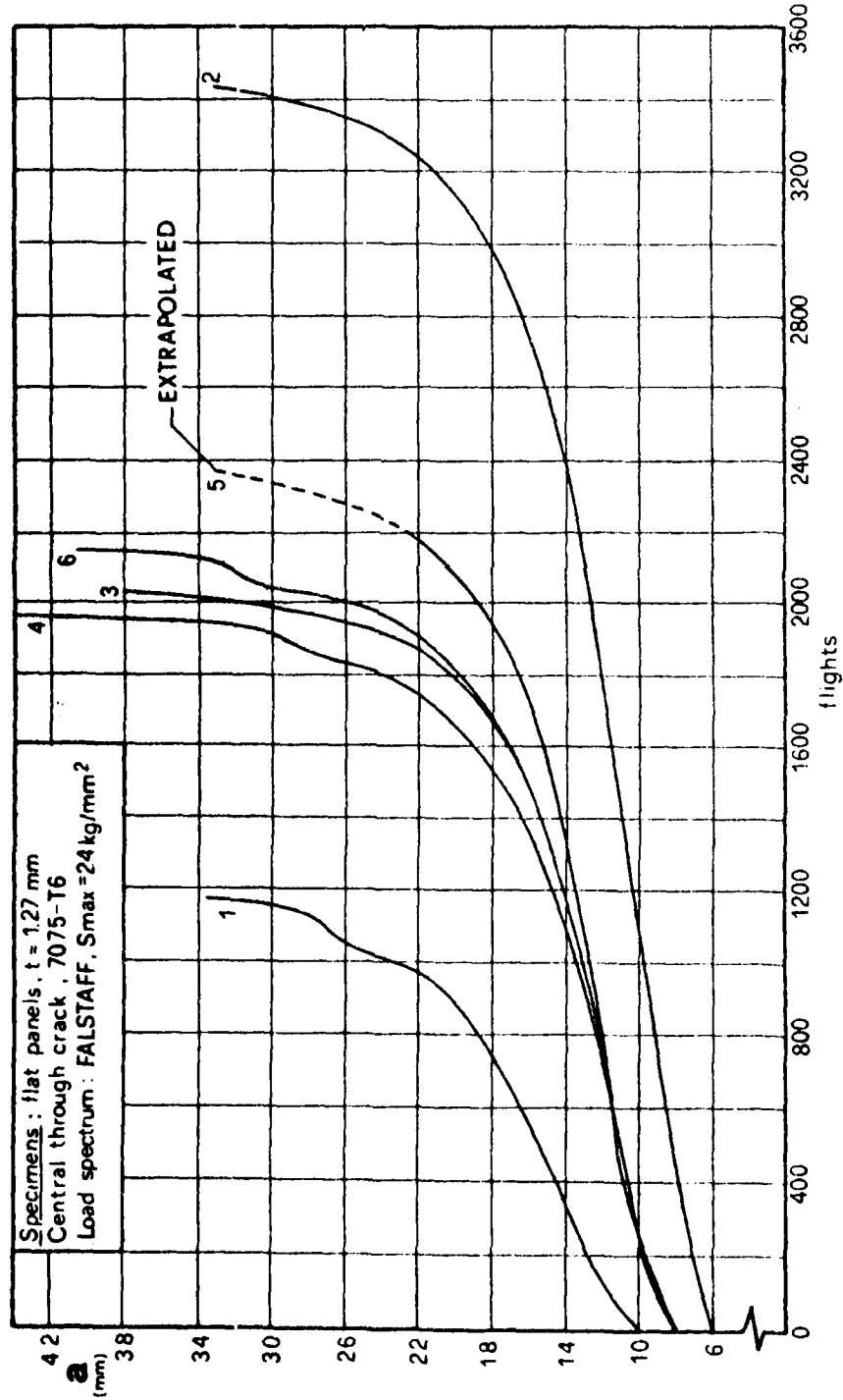


Fig. 6.a - Experimental results of flat panels tests under FALSTAFF spectrum loading with $S_{\text{max}} = 24 \text{ kg/mm}^2$.

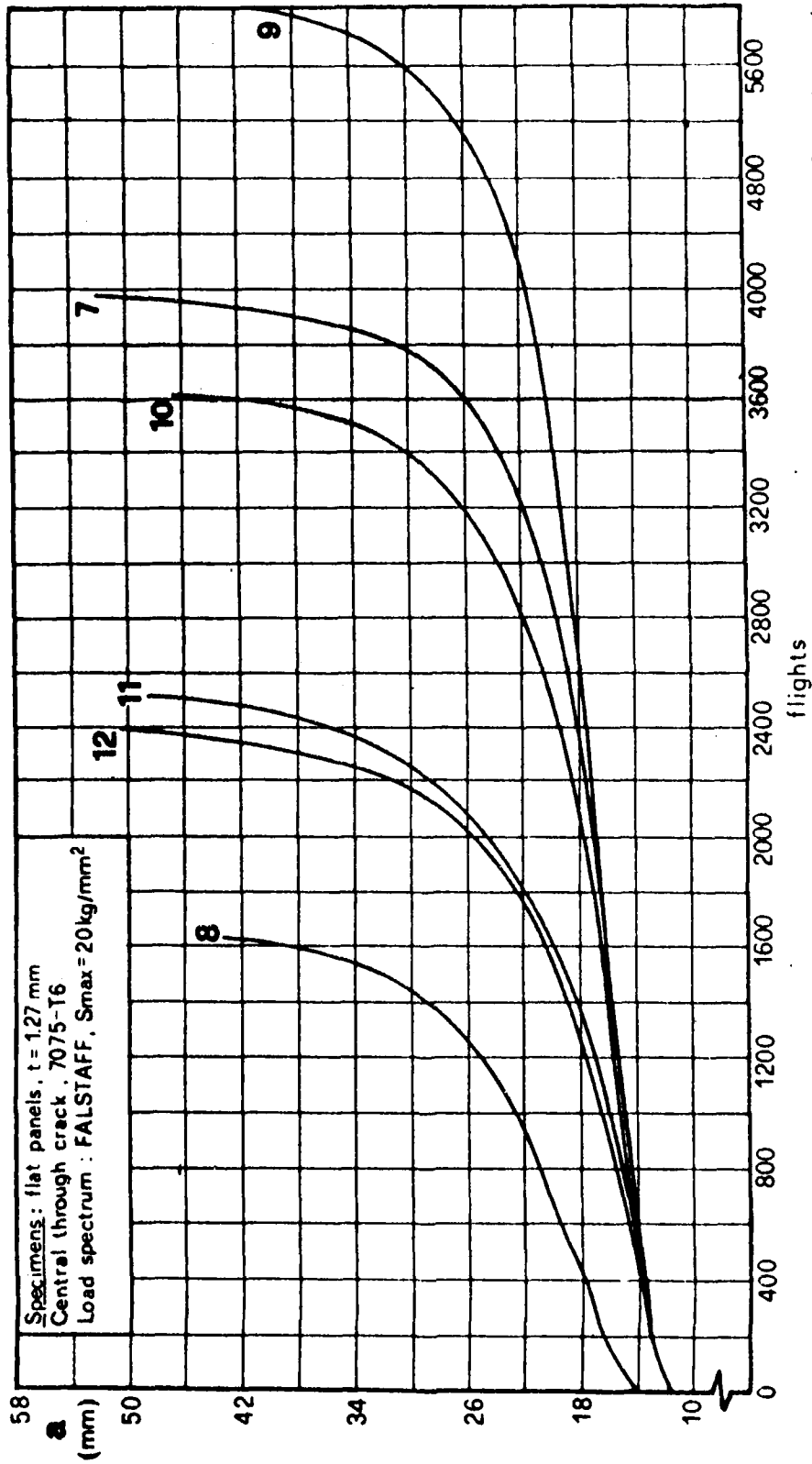


Fig. 6.b - Experimental results of flat panels tests under FALSTAFF spectrum loading with $S_{max} = 20 \text{ kg/mm}^2$.

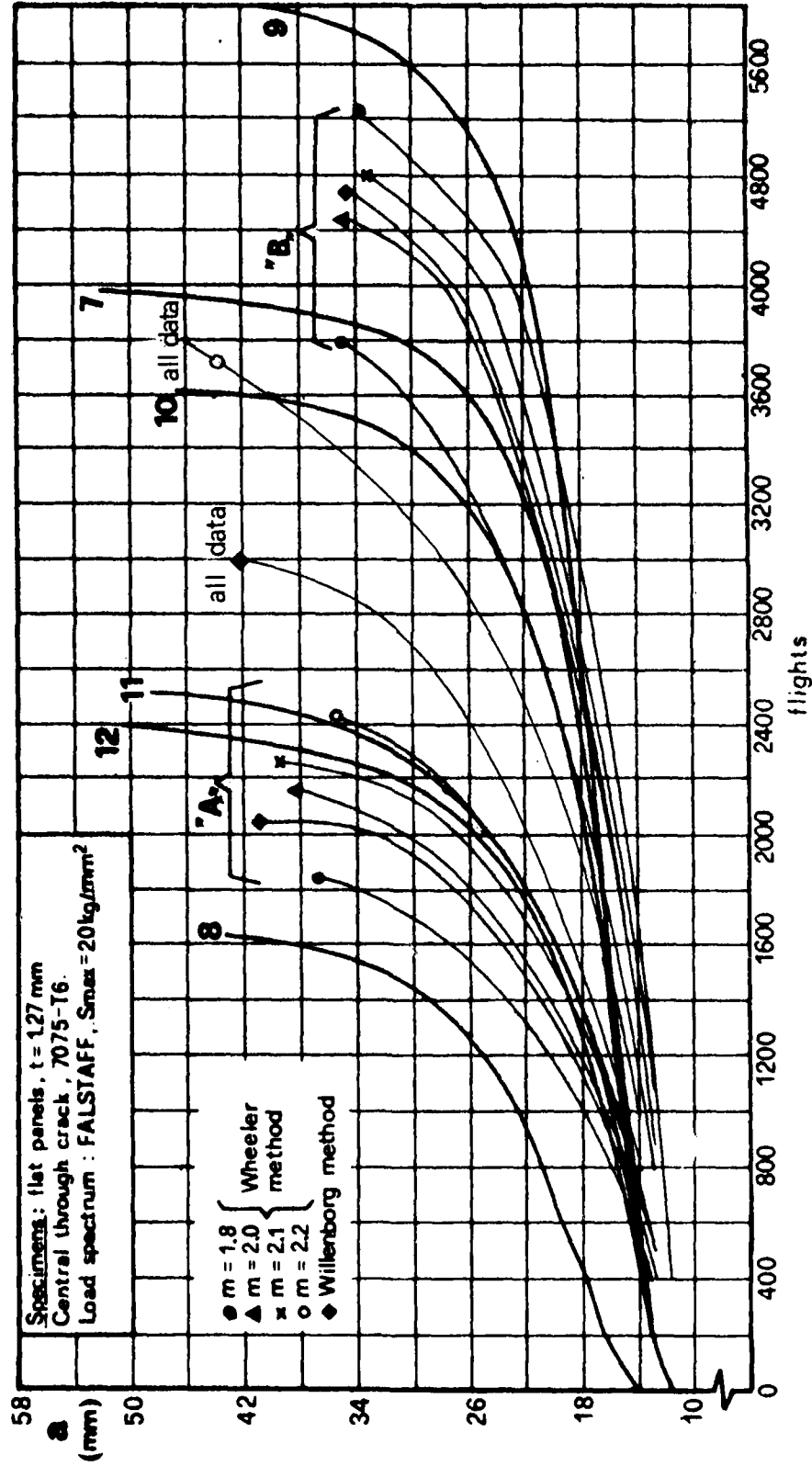


Fig. 7 - Comparison of experimental results with predictions obtained with the two sets of Forman law constants for flat panels tests under FALSTAFF spectrum with $S_{max} = 20 \text{ kg/mm}^2$. The curves "all data" are calculated with Forman law of Fig. 1.

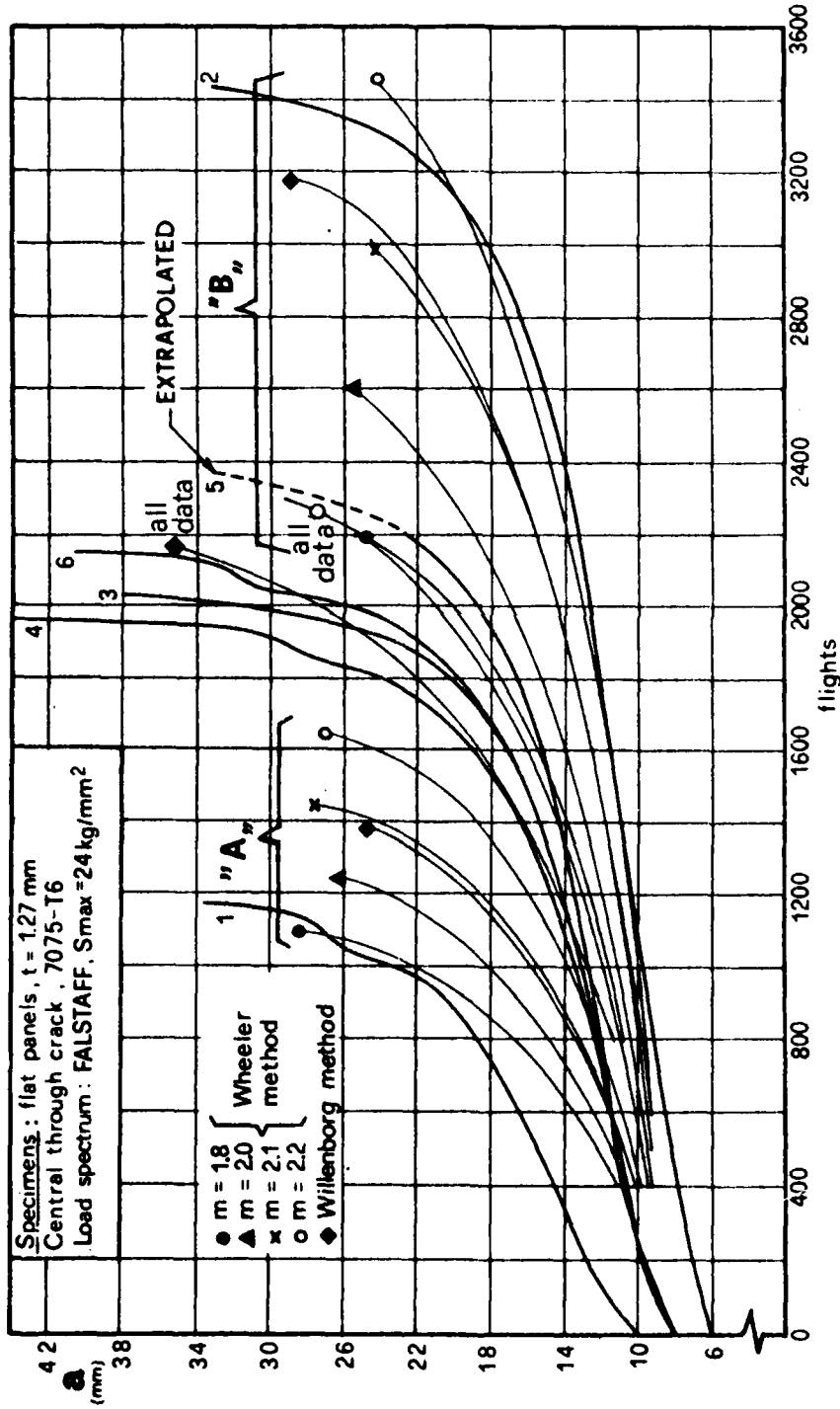


Fig. 7.a - Comparison of experimental results with predictions obtained with the two sets of Forman law constants for flat panels tests under FALSTAFF spectrum with $S_{max} = 24$ kg/mm². The curves "all data" are calculated with Forman law of Fig. 1.

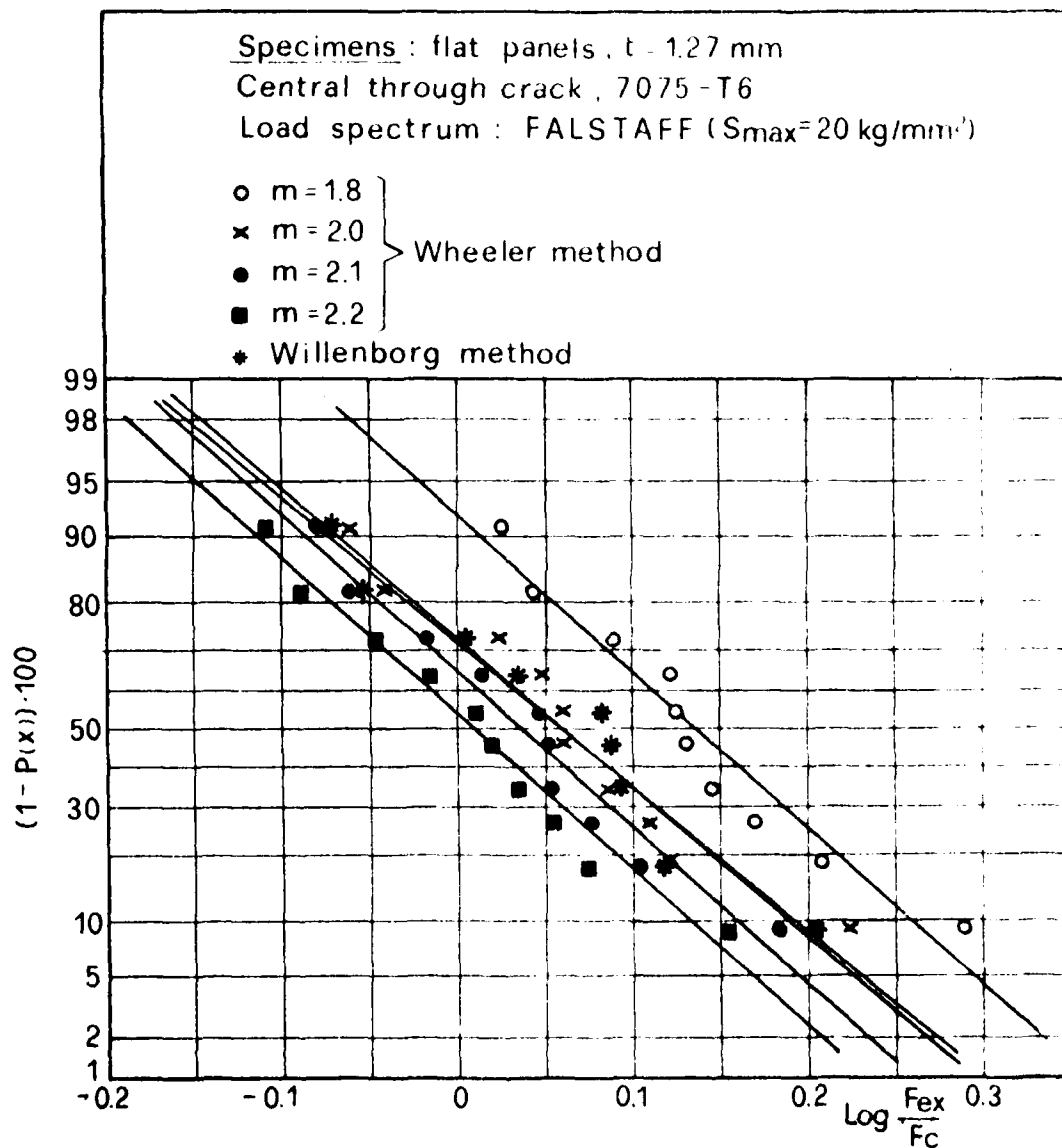


Fig.8.a - Lognormal cumulative distributions of the variable F_{ex}/F_c for flat panels tests under FALSTAFF Spectrum with $S_{\max} = 20 \text{ Kg/mm}^2$. F_c has been evaluated using Forman law constants of group 'A' or group 'B', as appropriate.

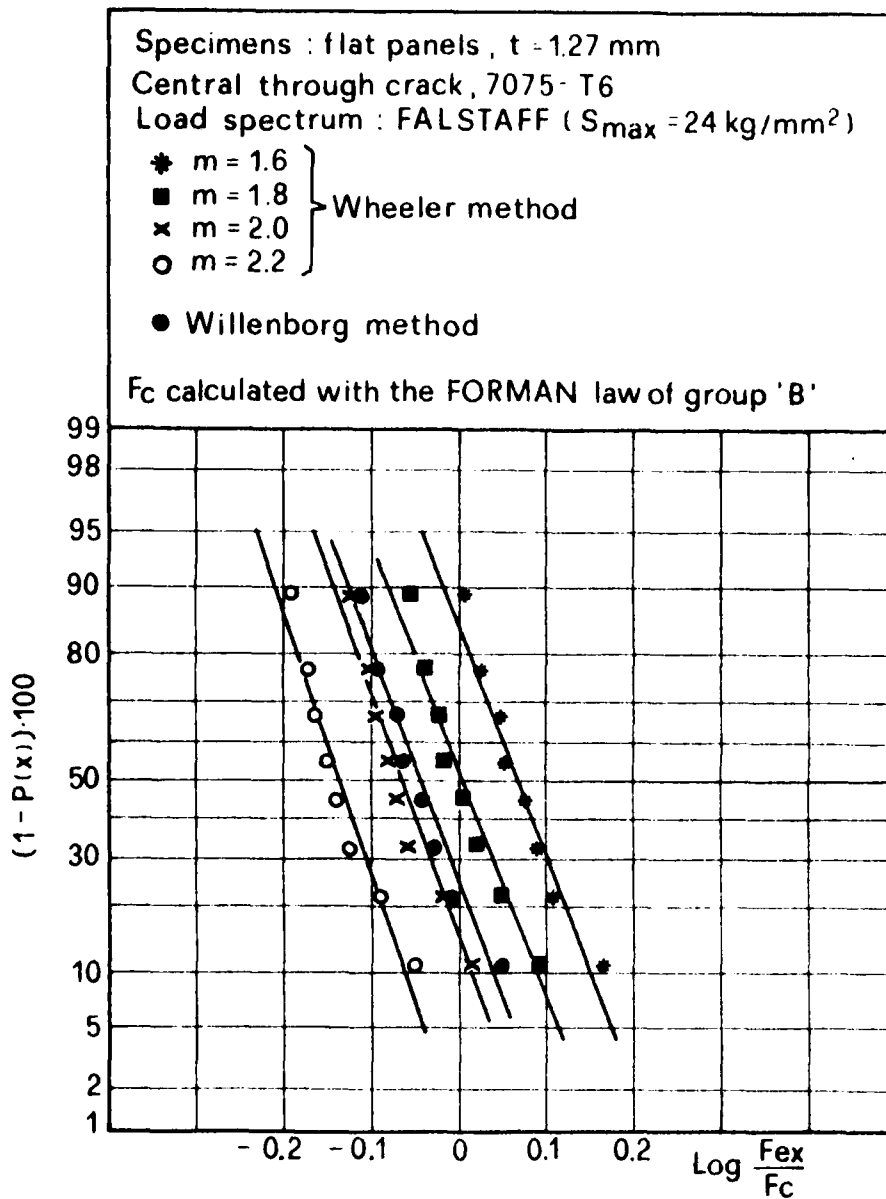


Fig. 8.b - Lognormal cumulative distributions of the variable F_{ex}/F_c for flat panels tests under FALSTAFF spectrum with $S_{\max} = 24 \text{ Kg/mm}^2$. F_c has been evaluated using Forman law constants of group 'B'.

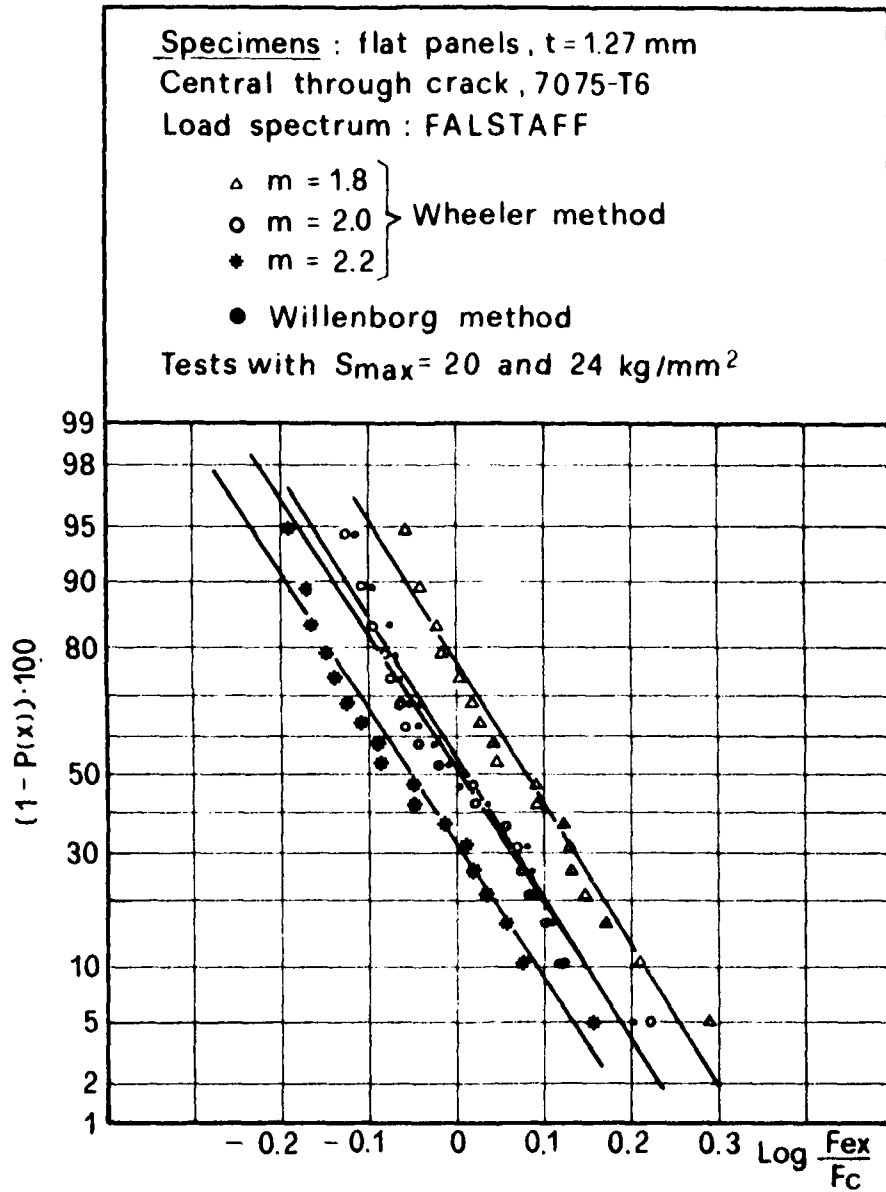


Fig. 8.c - Lognormal cumulative distributions of the variable F_{ex}/F_c for flat panels tests under FALSTAFF spectra with $S_{\max} = 20 \text{ kg/mm}^2$ and $S_{\max} = 24 \text{ kg/mm}^2$. F_c has been evaluated using Forman law constants of group 'A' or 'B', as appropriate

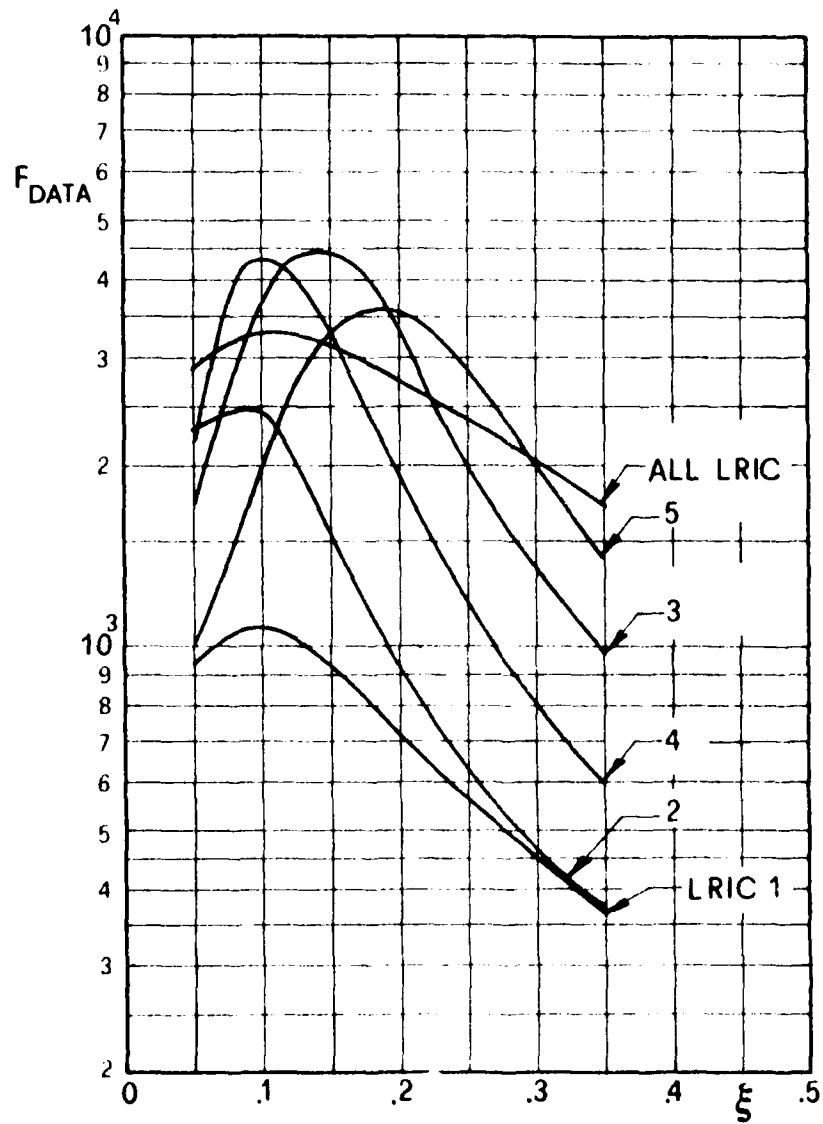


Fig. 9 - F_{DATA} versus flexibility parameter ξ for the constant amplitude-stiffened panels tests.

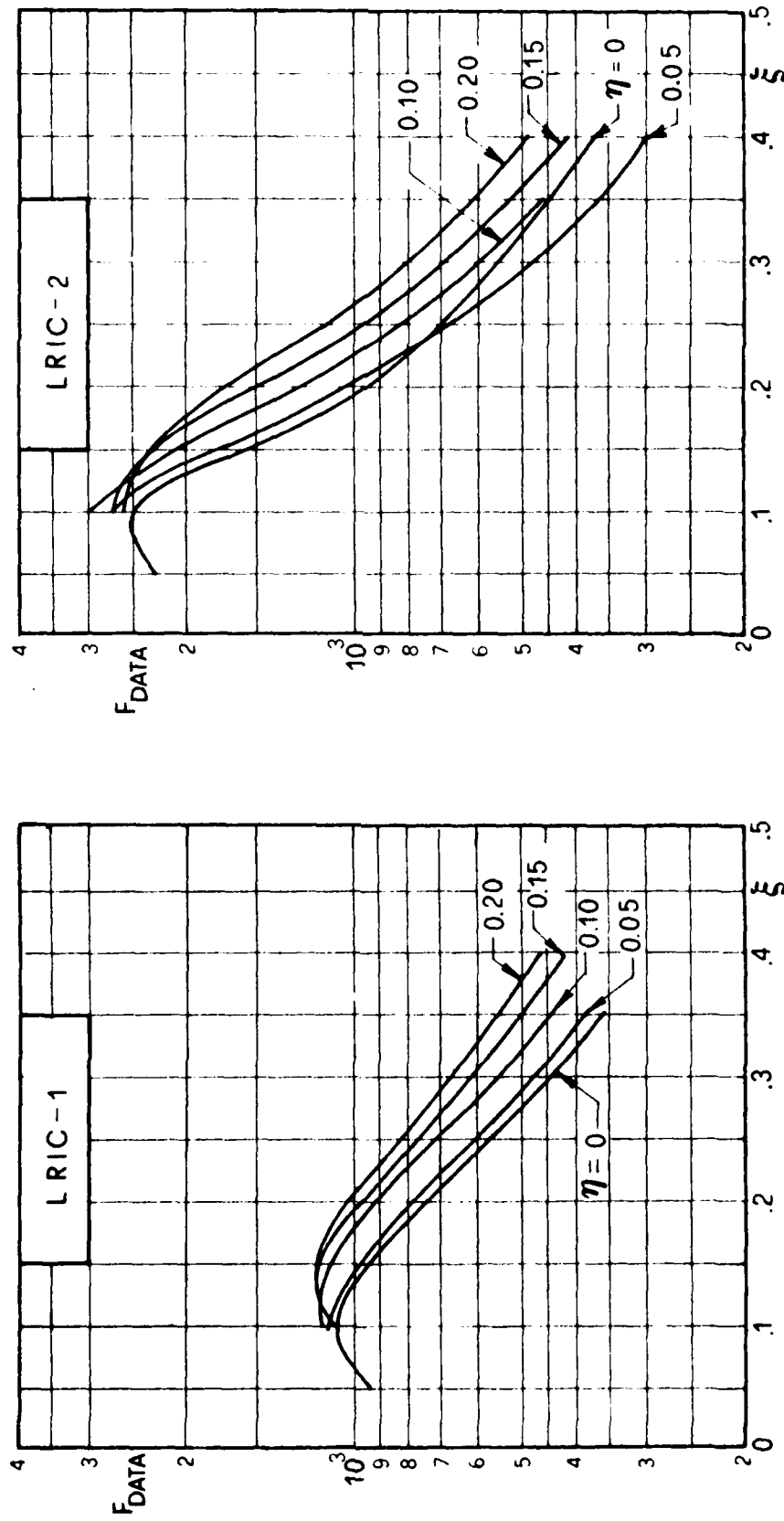


Fig. 10.a - F_{DATA} versus flexibility parameter ξ for the constant amplitude-stiffened panels tests, taking into account friction forces through the parameter η .

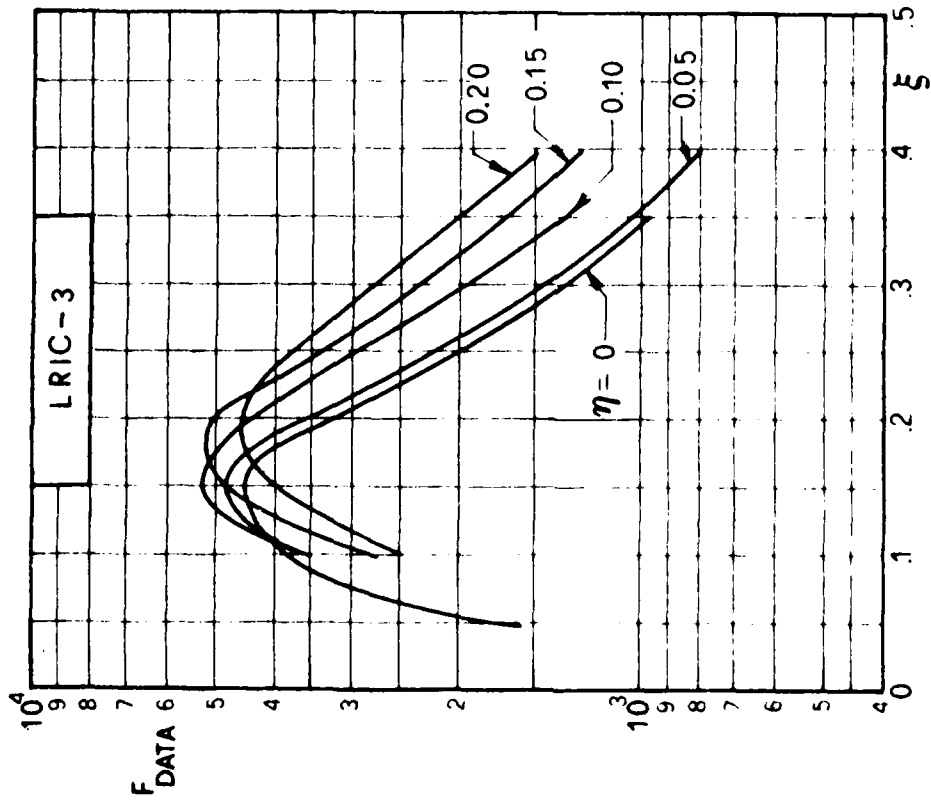
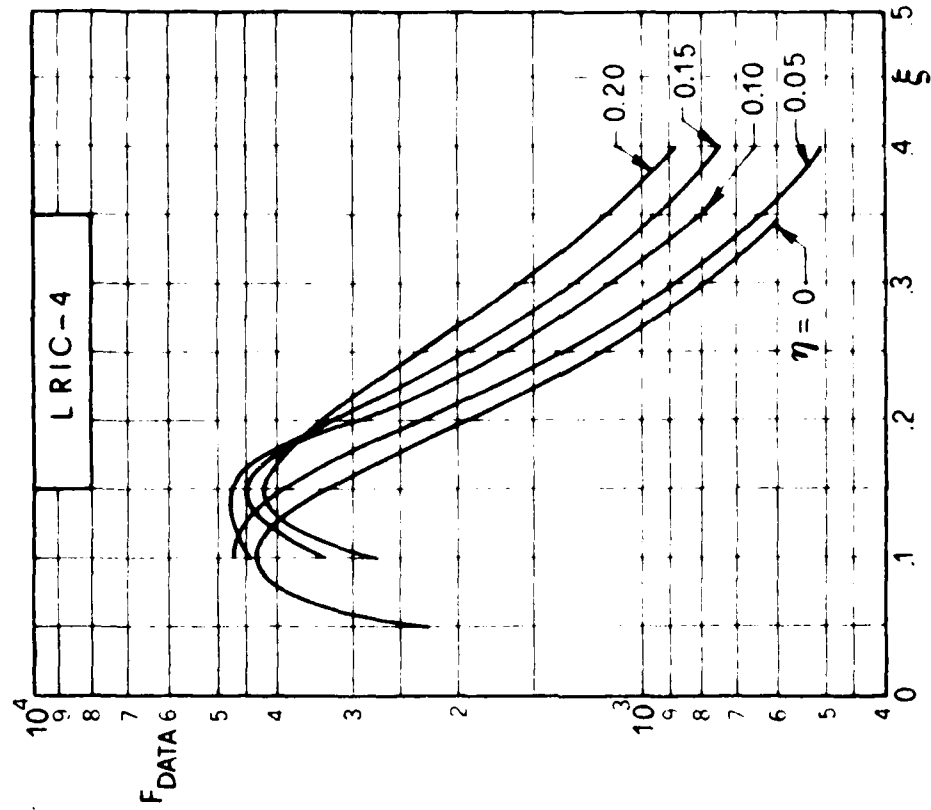


Fig. 10.b - Continued.

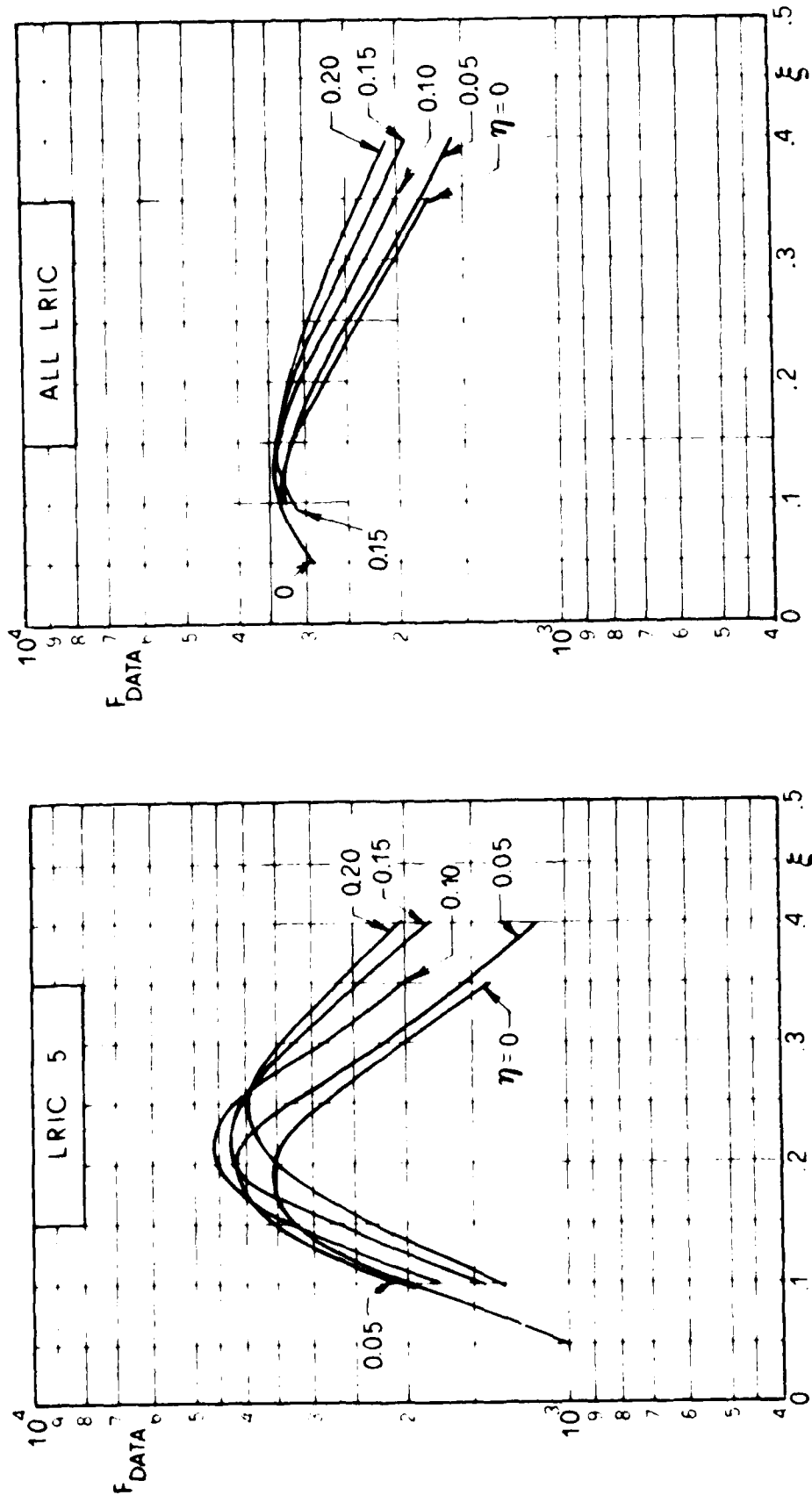


Fig. 10.c - Continued.

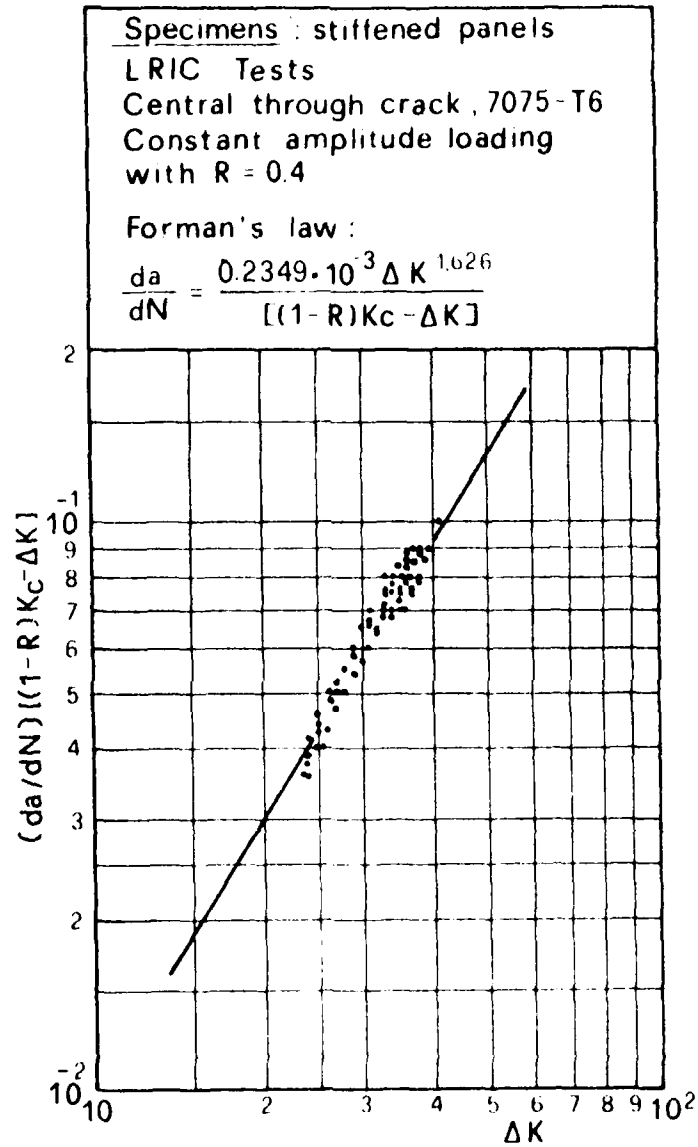


Fig. 11.a - Regression analysis of the experimental data from constant amplitude tests of the stiffened panels. ΔK has been evaluated using the best-fit value of the rivet flexibility parameter, $\xi = 0.10$.

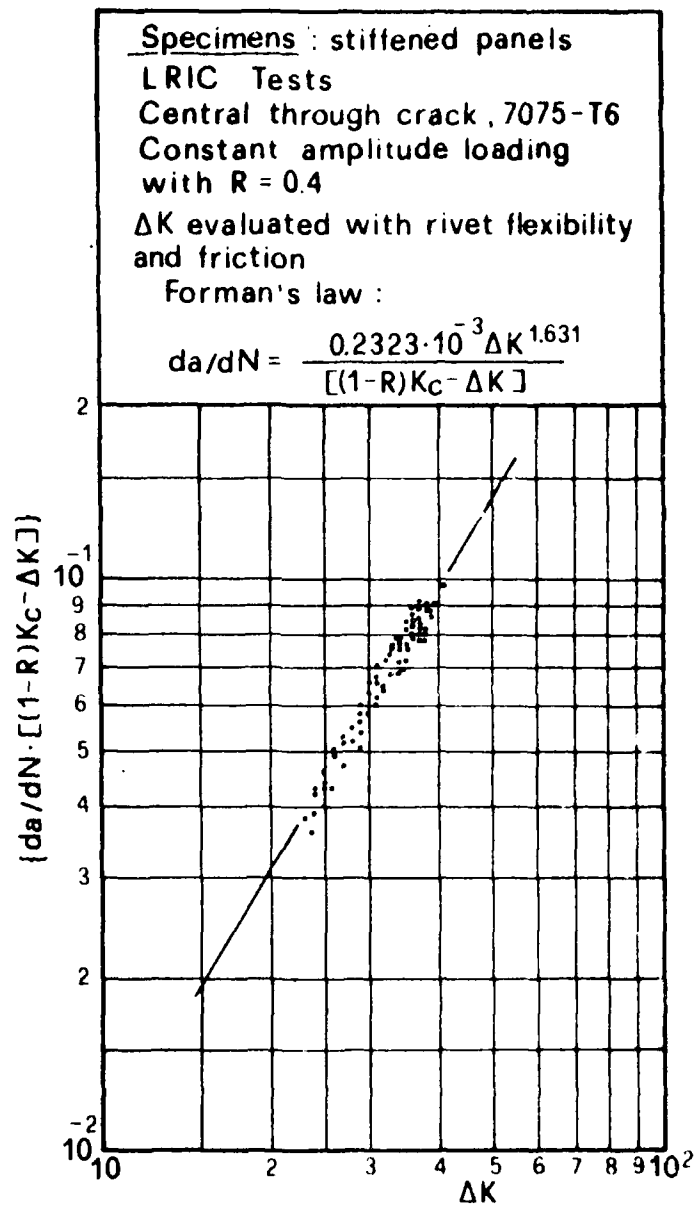


Fig. 11.b - Regression analysis of experimental data from constant amplitude tests of stiffened panels. ΔK has been evaluated using the best-fit values of the rivet flexibility parameter $\xi=0.15$ and friction parameter $\mu=0.10$.

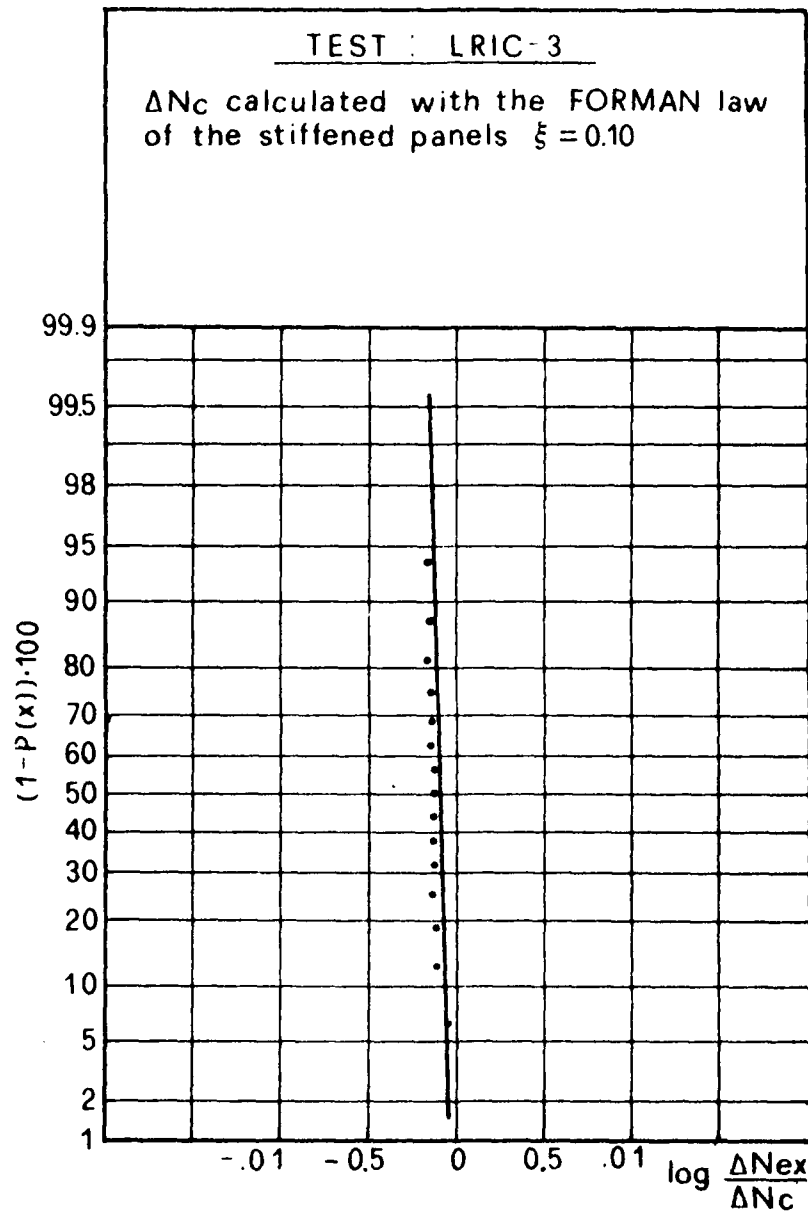


Fig. 12 - Lognormal cumulative distribution of the variable $\Delta N_{ex}/\Delta N_c$ for test LRIC-3. ΔN_c has been calculated with Forman law of the stiffened panels (Fig. 11.a) and assuming $\xi=0.10$.

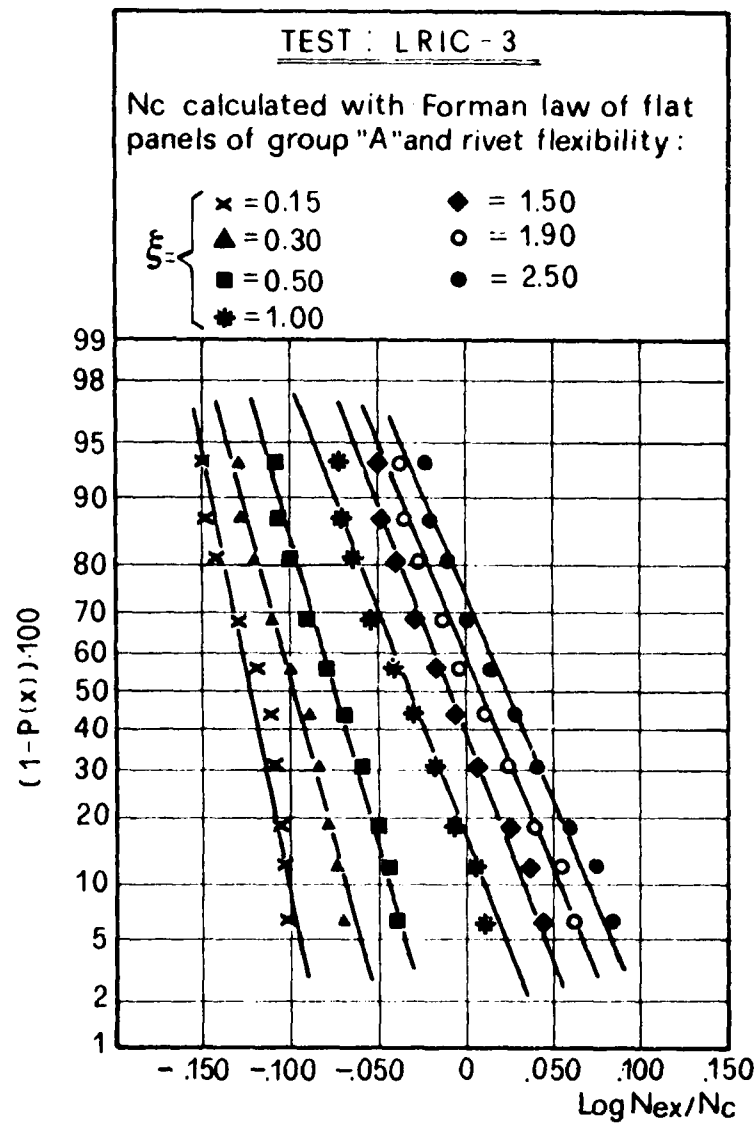


Fig. 13 - Lognormal cumulative distributions of the variable N_{ex}/N_c for test LRIC-3. N_c has been calculated using Forman law of group 'A' and ΔK evaluated using different values of ξ .

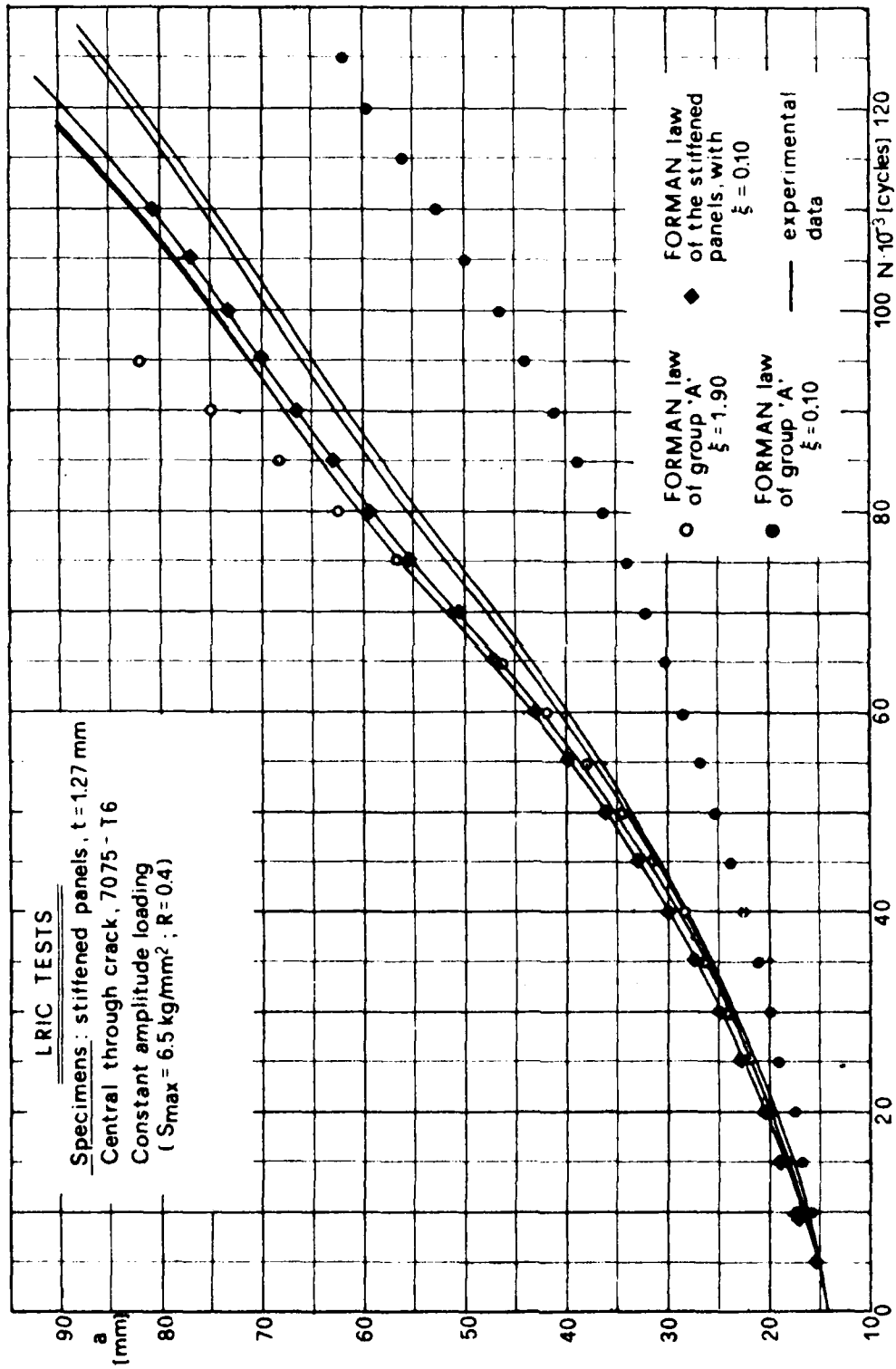


Fig. 14 - Comparison of the experimental data of the constant amplitude-stiffened panels tests with the predictions obtained using Forman law of group 'A' and ΔK evaluated using different values of ξ , rivet flexibility parameter.

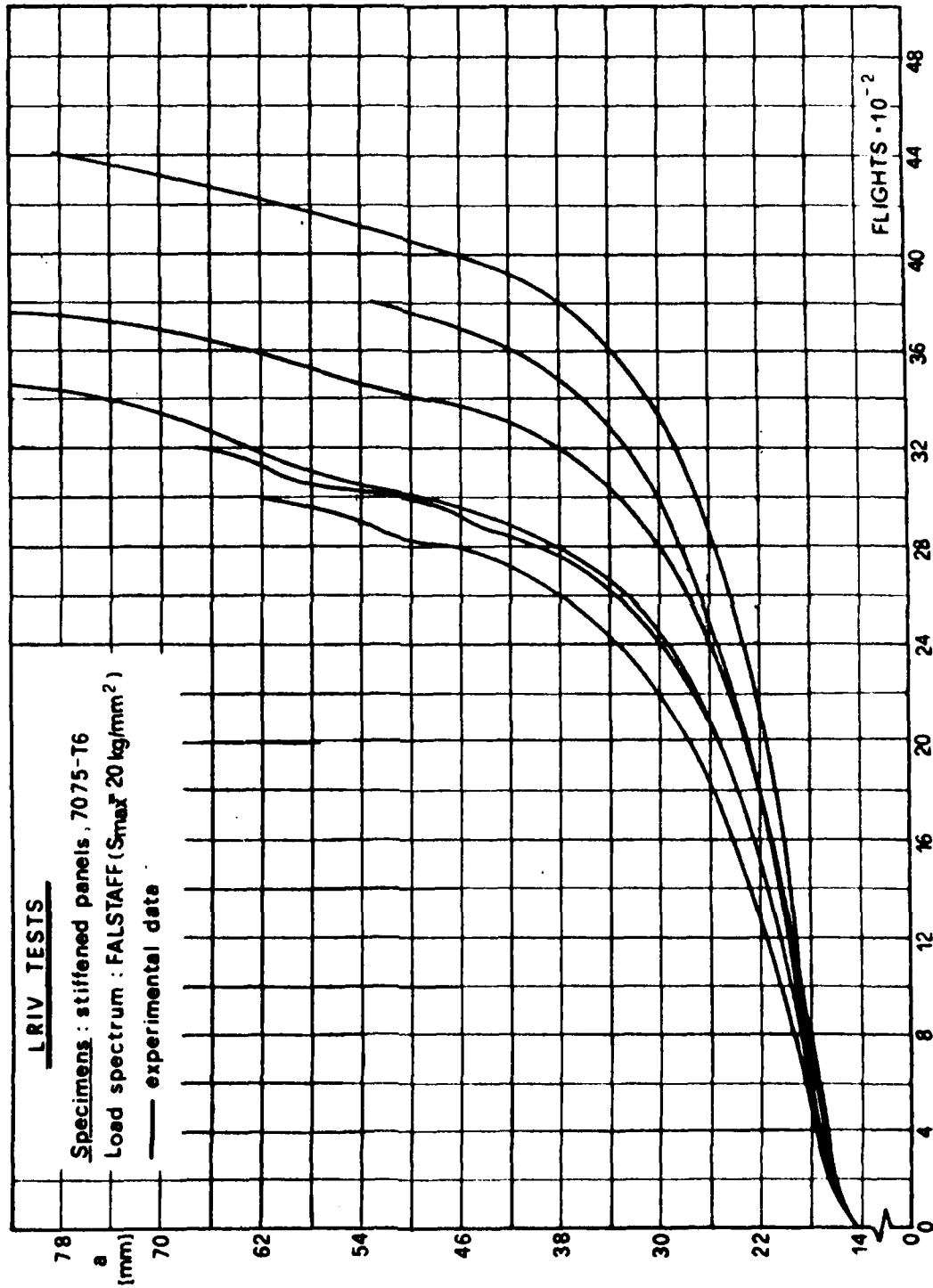


Fig. 15 - Experimental results of the variable amplitude tests of the stiffened panels.

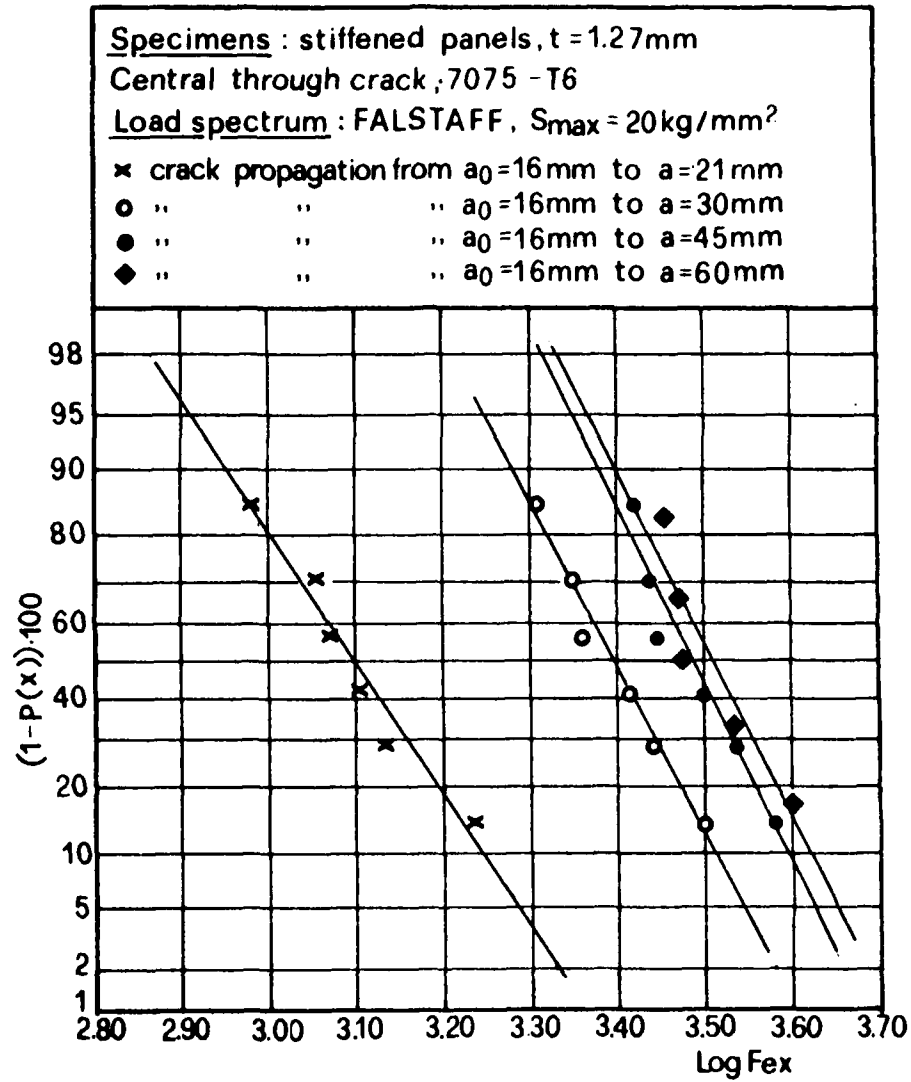


Fig. 16 - Lognormal cumulative distributions of the variable F_{ex} for the variable amplitude tests of the stiffened panels for four ranges of damage growth.

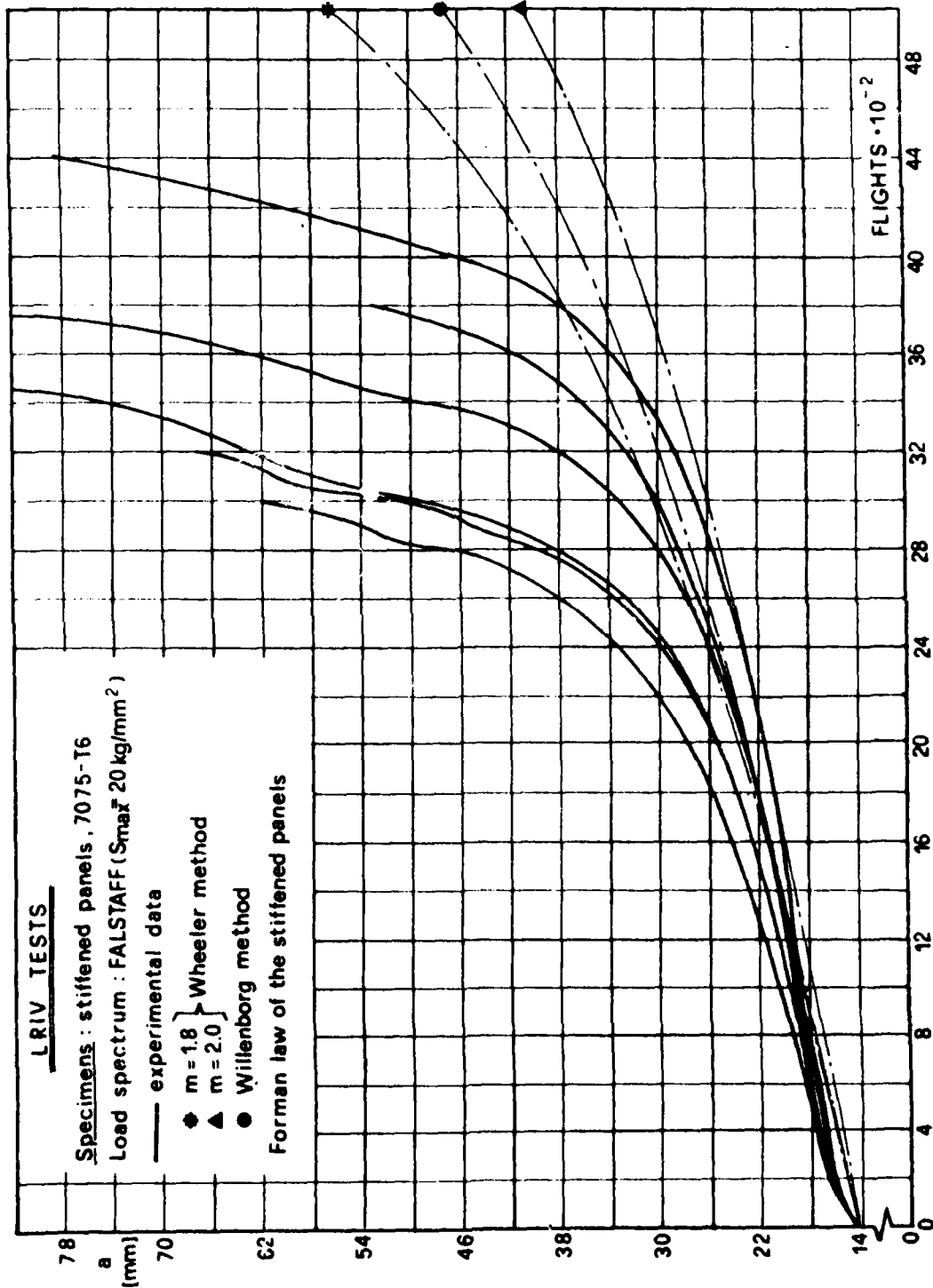


Fig. 17 - Comparison of the experimental data of the variable amplitude-stiffened panels tests with the predictions obtained using Forman law of the stiffened panels.

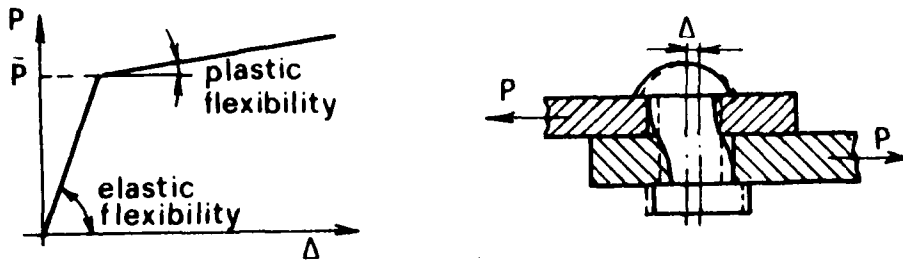


Fig.18.a

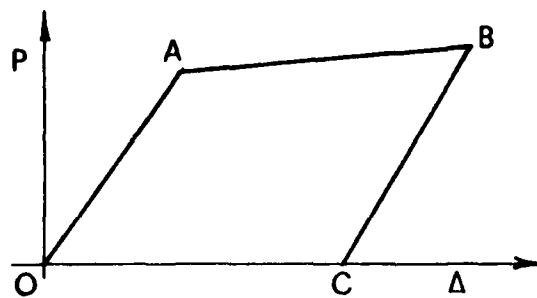


Fig.18.b

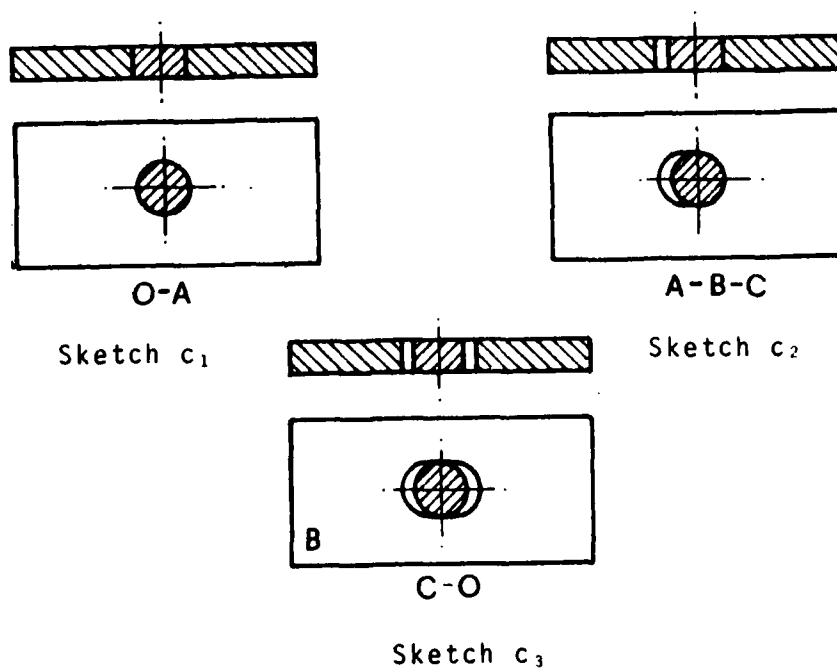


Fig.18.c

Fig. 18 - Schematic representation of a rivet-hole system behaviour.

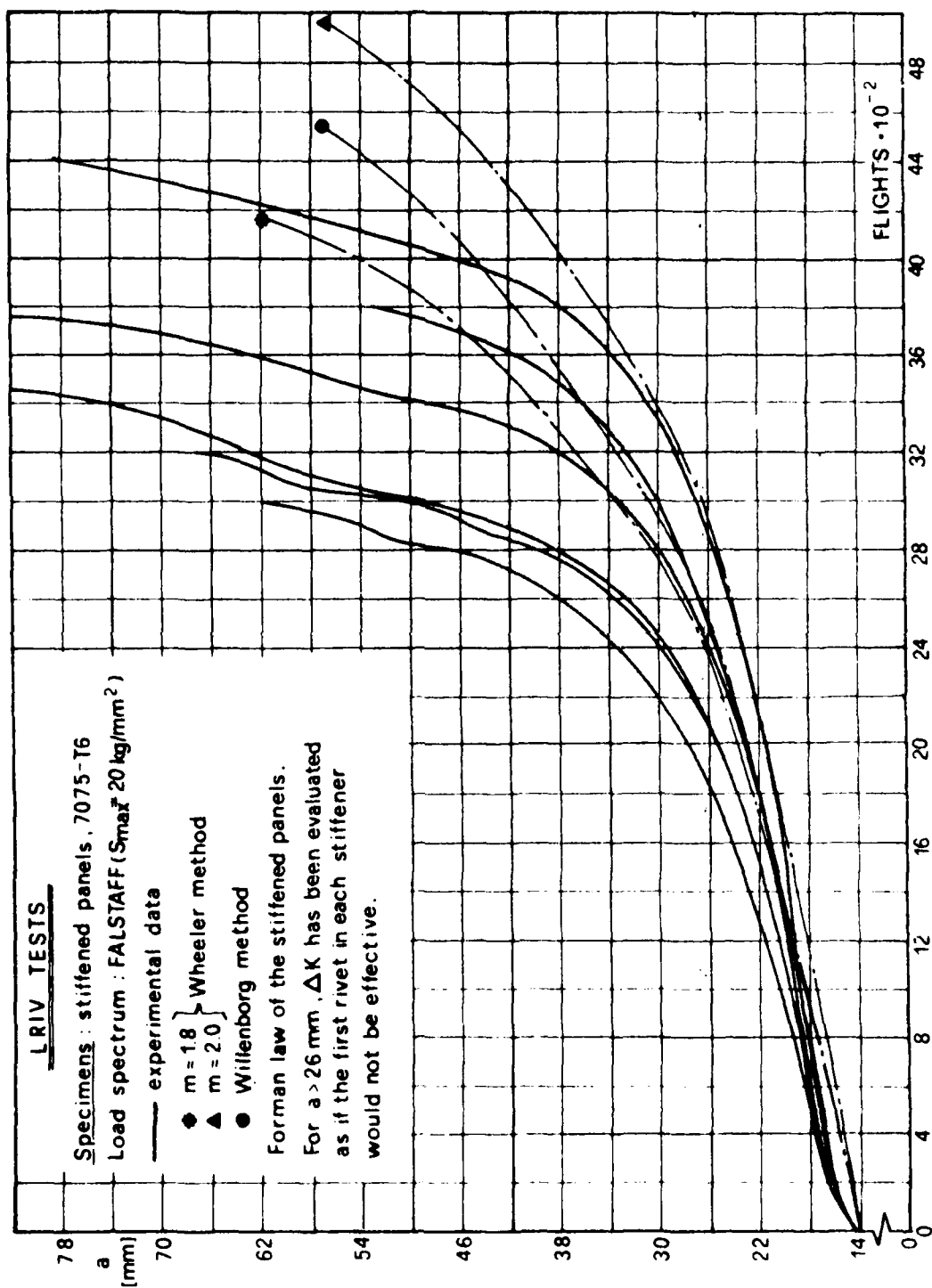
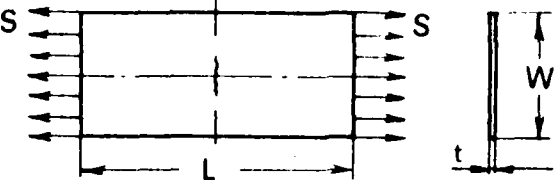
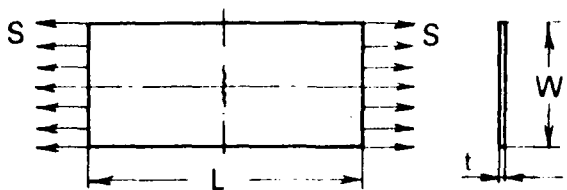


Fig. 19 - Comparison of the experimental data of the variable amplitude-stiffened panels tests with the predictions. The prediction curves are obtained using the Forman law of stiffened panels and ΔK evaluated, for $a > 26 \text{ mm}$, disregarding the actions of the first line of rivets immediately adjacent to the crack.

FLAT PANELS					
					
TYPE	W mm	L mm	t mm	n. panels	
				2024-T3	7075-T6
F1	400	500	1.27	0	10

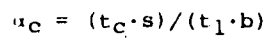
TEST	panel type	material	S _{max} kg/mm ²	R
LAZ-01	F1	7075-T6	9.00	0.00
LAZ-02	"	"	6.00	0.00
LAZ-03	"	"	6.00	0.20
LAZ-04	"	"	7.00	0.40
LAZ-05	"	"	7.00	0.60
LAZ-06	"	"	7.00	-0.50
LAZ-07	"	"	4.61	-1.00
LAZ-08	"	"	7.00	0.00
LAZ-09	"	"	5.09	-1.00
LAZ-10	"	"	7.00	0.70

Tab. 1.a - Main characteristics of the constant amplitude-flat panels tests.

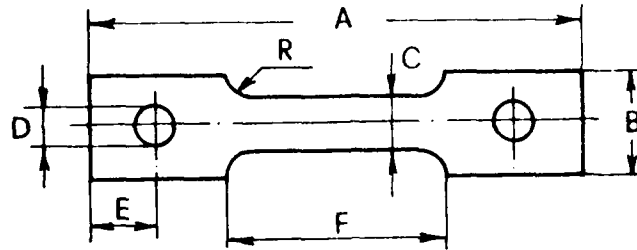
FLAT PANELS					
					
TYPE	W mm	L mm	t mm	n. panels	
				2024-T3	7075-T6
F ₁	400	500	1.27	0	12

TEST	panel type	a ₀ mm	spectrum	S _{ref} kg/mm ²	material
LRSV-1	F ₁	10.0	FALSTAFF	24.0	7075-T6
LRSV-2	"	6.0	"	"	"
LRSV-3	"	8.0	"	"	"
LRSV-4	"	8.0	"	"	"
LRSV-5	"	8.0	"	"	"
LRSV-6	"	8.0	"	"	"
LRSV-7	"	12.0	"	20.0	"
LRSV-8	"	14.0	"	"	"
LRSV-9	"	12.0	"	"	"
LRSV-10	"	12.0	"	"	"
LRSV-11	"	12.0	"	"	"
LRSV-12	"	12.0	"	"	"

Tab. 1.b - Main characteristics of the variable amplitude-flat panels tests.

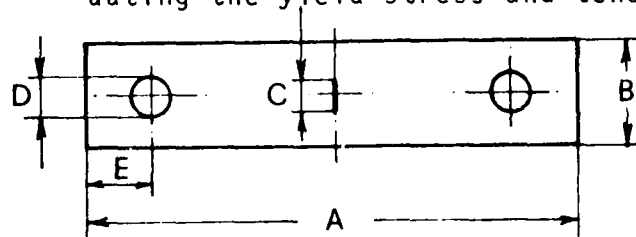


Tab. 1.c - Main characteristics of the constant amplitude stiffened panels tests.



TYPE	A mm	B mm	C mm	D mm	E mm	F mm	R mm
S ₁	360	74	38	27	55	157	40

Tab.2.a - Dimensions of the specimens used for evaluating the yield stress and tensile strength.



TYPE	A mm	B mm	C mm	D mm	E mm
S ₂	360	74	30	27	55

Tab.2.b - Dimensions of the specimens used for K_C evaluation.

Test LAZ-07		Test LAZ-09	
a	cycles	a	cycles
7.6	79770.	5.6	21515.
9.1	94770.	6.1	26085.
9.4	97830.	6.6	29785.
9.9	101040.	7.2	33170.
10.4	103960.	7.6	35935.
10.9	106515.	8.6	40330.
11.8	111240.	9.4	44850.
12.1	112880.	10.5	49330.
12.5	114505.	11.5	52625.
13.6	117735.	12.1	53935.
14.1	119850.	12.6	55365.
14.9	122065.	13.1	57005.
15.4	123945.	13.7	58825.
16.0	125585.	14.1	59965.
16.6	127290.	14.9	61510.
17.1	129140.	15.4	62980.
17.9	130665.	16.0	64425.
18.4	132045.	16.6	65790.
19.0	133580.	17.4	67165.
19.8	135390.	17.8	68195.
20.7	137565.	18.6	69315.
21.6	139350.	19.5	71385.
22.3	140780.	20.1	72655.
22.9	142095.	20.6	73535.
23.5	143185.	21.0	74125.
24.1	144465.	21.6	75040.
25.5	146750.	22.3	76560.
26.0	147550.	22.8	77480.
26.5	148395.	23.6	78755.
27.0	149355.	24.5	79955.
28.3	151565.	26.2	82745.
28.9	152530.	27.3	84360.
29.5	153490.	28.0	85405.
30.5	154950.	29.0	86860.
31.7	156760.	29.9	87685.
32.5	157855.	30.6	88885.
33.4	159125.	31.4	89820.
34.7	161120.	32.2	90870.
35.5	162280.	33.1	91950.
36.7	163760.	34.0	93015.
37.4	164680.	34.8	93775.
		36.8	95775.
		37.7	96745.
		39.3	98775.

Tab. 3 - Results of constant amplitude-flat specimens tests.

Test LAZ-06

a	cycles
9.5	12665.
10.3	15135.
10.9	16195.
11.4	17185.
12.0	18770.
13.9	22360.
14.6	23810.
15.4	24930.
16.1	25960.
17.0	27170.
17.8	28230.
19.0	29640.
19.6	30400.
20.5	31340.
21.0	31895.
21.5	32535.
22.3	33240.
22.9	34000.
23.5	34760.
24.3	35400.
25.1	36040.
25.6	36480.
26.4	37080.
27.3	37770.
28.0	38235.
28.7	38830.
30.0	39850.
30.7	40445.
31.3	40910.
32.0	41370.
32.6	41810.
33.3	42185.
34.2	42725.
34.8	43125.
35.4	43455.

Test LAZ-02

a	cycles
8.6	49015.
8.9	50270.
9.4	51415.
10.6	54980.
11.1	56400.
12.0	59255.
13.1	62155.
13.6	63185.
13.9	63915.
14.9	66195.
15.6	67635.
16.1	68700.
17.0	70790.
17.5	72155.
18.1	73405.
19.4	75520.
20.1	76365.
20.6	77440.
21.4	78470.
21.9	79435.
22.5	80330.
23.1	81390.
23.6	82210.
24.6	83400.
25.9	84900.
27.0	86550.
27.9	87635.
28.4	88135.
29.0	88930.
29.5	89685.
31.4	91510.
32.3	92455.
33.2	93190.
34.1	94075.
34.8	94790.
35.5	95310.
37.0	96715.
38.0	97485.
39.0	98270.
39.9	98900.
41.3	99775.
43.2	101055.
44.5	101750.

Tab. 3 - Continued.

Test LAZ-08		Test LAZ-01	
a	cycles	a	cycles
4.2	11570.	4.1	6745.
4.5	13455.	4.7	7735.
4.8	15290.	5.1	8795.
5.2	17290.	5.8	10055.
6.2	21340.	6.4	10980.
6.7	22785.	7.1	11945.
7.1	24735.	7.6	13000.
7.7	26595.	8.6	14515.
8.7	29815.	9.9	15775.
9.4	31290.	10.3	16375.
10.3	33960.	11.1	17230.
11.1	35475.	11.6	17755.
11.5	36470.	12.6	18695.
12.3	37615.	13.1	19150.
12.8	38545.	13.7	19640.
13.3	39550.	14.2	20170.
14.0	40705.	14.8	20665.
15.5	42955.	15.5	21170.
16.0	43840.	16.5	21940.
16.6	44620.	17.1	22335.
17.3	45415.	18.1	22985.
18.0	46275.	19.1	23590.
18.6	47120.	20.0	24170.
19.4	47950.	20.9	24670.
20.0	48665.	21.8	25065.
20.8	49435.	22.8	25600.
21.4	50030.	23.6	25925.
22.3	50890.	24.4	26215.
22.9	51495.	25.1	26480.
24.0	52595.	26.1	26775.
24.6	53100.	26.9	27050.
25.4	53695.	27.9	27330.
26.1	54275.	28.8	27590.
26.9	54825.	29.9	27870.
27.6	55350.	31.2	28170.
29.1	56355.	32.6	28435.
29.8	56830.	34.0	28675.
30.5	57300.	35.3	28910.
31.3	57805.	36.8	29150.
32.0	58230.	38.7	29405.
33.2	58850.	40.9	29700.
34.2	59370.		
34.9	59755.		
35.8	60155.		

Tab. 3 - Continued.

Test LAZ-03

a	cycles
8.2	68065.
8.6	69870.
8.9	71490.
9.3	73485.
9.6	75815.
12.6	84365.
14.0	88420.
14.4	89880.
16.1	94140.
17.0	95555.
17.6	97110.
18.2	98750.
19.0	100655.
19.9	101890.
20.6	103295.
21.5	105175.
22.7	106790.
23.4	108065.
24.3	109690.
25.9	111420.
27.2	113625.
28.2	115400.
29.8	116835.
31.0	118325.
32.0	119445.
33.0	120530.
34.8	122530.
36.9	124685.
38.8	126370.
39.8	127165.
40.9	128240.
41.8	128730.
42.7	129500.
43.8	130375.
45.2	131370.
45.8	131860.
46.9	132630.
48.3	133465.
49.2	134040.

Test LAZ-04

a	cycles
11.6	4665.
13.1	9130.
13.9	11355.
14.6	13665.
15.1	15265.
15.8	16535.
16.4	18060.
17.0	19250.
17.9	21145.
18.7	23015.
19.4	24490.
20.1	25840.
20.7	26895.
22.1	29330.
23.0	31075.
23.5	31850.
24.3	33070.
25.0	34260.
25.9	35520.
26.6	36545.
27.4	37585.
28.3	38865.
28.8	39605.
29.5	40510.
30.1	41360.
31.1	42460.
32.0	43530.
32.8	44540.
33.7	45520.
34.6	46420.
35.5	47325.
36.8	48675.
37.7	49490.
40.4	51545.
40.8	52030.
41.4	52620.
42.7	53510.
43.6	54225.
44.1	54555.
44.6	54930.
45.5	55680.
46.7	56410.

Tab. 3 - Continued.

Test LAZ-05

a	cycles
17.6	23710.
18.4	27825.
18.7	29825.
19.4	33145.
20.1	37220.
21.5	44550.
22.3	46970.
23.4	50420.
24.2	54125.
25.5	59775.
25.9	61355.
26.7	65045.
27.3	66550.
27.6	68120.
28.4	71100.
29.0	73570.
30.5	77405.
31.0	78945.
31.4	80010.
32.0	81955.
32.7	84355.
34.0	87230.
34.8	88630.
35.5	90450.
36.3	93105.
36.8	94070.
37.3	95470.
37.8	96555.
38.3	97480.
38.7	98405.
39.2	99550.
39.5	100210.
40.0	101175.
40.4	102275.
40.9	103390.
41.3	104215.
41.8	105080.
42.3	106015.
43.0	107385.

Test LAZ-10

a	cycles
21.3	12585.
21.6	14500.
21.9	16270.
22.3	18905.
22.8	22610.
23.2	25465.
23.8	28990.
24.0	30655.
24.4	32860.
25.0	36745.
25.4	38735.
25.7	41255.
26.1	43420.
26.5	45635.
26.9	47380.
27.2	49495.
27.6	51295.
27.9	52935.
28.3	54705.
28.9	58075.
29.3	59745.
29.6	61355.
30.0	63135.
30.3	64750.
30.7	66365.
31.0	68080.
31.5	70010.
31.9	71625.
32.5	74395.
33.2	76895.
33.6	78755.
34.3	81445.
34.9	83955.
35.5	86050.
36.0	88240.
36.5	89960.
37.0	91610.
37.6	93310.
38.0	94525.
38.3	95785.
39.0	97915.
39.5	99460.

Tab. 3 - Continued.

[illegible][illegible][illegible]

Tab. 4 - Results of the variable amplitude-flat panels tests.

[illegible][illegible][illegible]

Tab. 4 - Continued.

TEST LRSV 7	
FLIGHTS	α (mm)
0	11.05
100	12.10
201	12.65
306	12.95
401	13.25
501	13.55
602	13.80
700	13.95

900	14.45
1000	14.65
1105	14.80
1200	15.10
1302	15.30
1400	15.75
1503	15.80
1600	16.00
1705	16.25
1800	16.50
1900	16.85
2000	17.05
2100	17.25
2200	17.55
2302	17.75
2400	18.05
2501	18.50
2600	18.85

2800	19.40
2900	19.90
3000	20.60
3109	21.10
3200	21.75
3300	22.70
3400	23.70
3500	24.75
3600	25.95
3700	27.85
3800	31.20
3900	37.50
3940	43.45
3960	50.45

TEST LRSV 9	
FLIGHTS	α (mm)
0	11.20
100	12.35
200	12.80
300	13.20
400	13.60
500	13.90
600	14.15
700	14.40
800	14.55
900	14.75
1000	15.00
1100	15.15
1200	15.35
1300	15.50
1400	15.70
1500	15.95
1600	16.15
1700	16.35
1800	16.55
1900	16.75
2000	16.80
2100	16.95
2200	17.15
2300	17.30
2400	17.50
2500	17.65
2600	17.85
2700	18.00
2800	18.25
2900	18.50
3000	18.70
3100	18.95
3200	19.20
3300	19.50
3400	19.75
3500	19.95
3600	20.15
3700	20.35
3800	20.70
3900	21.10
4000	21.70
4100	22.30
4200	22.90
4300	23.65

[illegible]

Tab. 4 - Continued.

[illegible][illegible][illegible]

Tab. 4 - Continued.

Test LRIC-1		Test LRIC-2	
a	cycles	a	cycles
19.6	19440.	18.1	15290.
20.8	21805.	19.0	17900.
22.5	26730.	20.0	20525.
23.4	28385.	21.6	24645.
24.3	30190.	23.6	29005.
25.1	32480.	24.6	31320.
27.3	36405.	27.2	35925.
29.9	41275.	29.1	39280.
31.1	43515.	30.3	41660.
32.6	45890.	31.3	43195.
35.3	50640.	32.7	45260.
36.7	52555.	34.1	47380.
40.3	56695.	37.7	52615.
42.3	59705.	39.5	55030.
44.5	62195.	41.1	57245.
48.5	66940.	43.0	59440.
50.0	68370.	44.8	61595.
51.3	70295.	46.2	63045.
52.8	72025.	47.2	64090.
55.7	75615.	48.1	65295.
56.9	76840.	49.0	66370.
58.2	78360.	50.4	67930.
59.3	79510.	51.1	68725.
60.5	81230.	52.3	70145.
61.5	82625.	53.3	71280.
63.6	85620.	54.5	72700.
66.3	89880.	55.5	73925.
67.4	91180.	57.8	76515.
68.6	92510.	58.8	77770.
70.7	95415.	59.9	78990.
72.3	98070.	60.8	80335.
74.8	101345.	61.7	81345.
76.3	103350.	64.0	84370.
78.1	105345.	65.7	86705.
79.3	107180.	66.7	88165.
79.8	108380.	67.8	89835.
80.9	109755.	68.9	91135.
81.8	110680.	71.1	94490.
82.9	112285.	72.6	96480.
83.9	113405.	73.4	97840.
85.0	114590.	74.6	99510.
86.3	116195.	78.8	105075.
87.2	117280.	80.1	106630.
88.7	118990.	81.5	108325.
90.0	120105.	83.3	110445.

Tab. 5 - Results of the constant amplitude-stiffened panels tests.

Test LRIC-3		Test LRIC-4	
a	cycles	a	cycles
16.1	7710.	17.1	10505.
18.6	15425.	17.8	12810.
19.3	16690.	19.4	17325.
20.2	19380.	20.0	19525.
20.6	20715.	20.8	21740.
22.3	24240.	21.5	23955.
22.7	25305.	23.5	28495.
23.2	26695.	25.3	32635.
23.9	27935.	26.1	34910.
24.5	29375.	27.1	37000.
25.2	30685.	29.6	41950.
25.8	31835.	30.9	44115.
26.3	32905.	32.3	46750.
27.7	35845.	33.4	48875.
29.8	39275.	34.6	50815.
31.0	41475.	35.5	52340.
32.7	44255.	36.5	53840.
34.0	46465.	37.7	55840.
35.4	48670.	38.7	57200.
38.2	51865.	40.0	58960.
39.5	54565.	42.0	62145.
40.9	56470.	44.1	64785.
42.7	58660.	47.6	69445.
44.5	60860.	49.0	71365.
45.7	62505.	50.9	73870.
47.7	65005.	53.6	77165.
49.8	67275.	55.7	79715.
51.8	69550.	57.7	82380.
53.7	71585.	59.4	84840.
55.4	73645.	61.0	87005.
57.0	75465.	62.6	89445.
58.5	77270.	64.1	91690.
60.4	79695.	65.3	93705.
61.5	81105.	67.0	96215.
62.2	82055.	68.7	98745.
63.2	83290.	70.1	100940.
65.2	86205.	71.3	102795.
66.0	87235.	72.7	104985.
66.8	88425.	73.8	106690.
67.7	89655.	74.9	108125.
69.5	92360.	75.9	109850.
70.8	93945.	77.1	111665.
71.7	95205.	77.9	113010.
72.9	97015.	79.4	115010.
75.4	100280.	80.8	116790.

Tab. 5 - Continued.

Test LRIC-5

a	cycles
17.4	11650.
18.0	13705.
18.7	16005.
20.4	20745.
21.1	22800.
23.1	27970.
23.9	29880.
25.0	32435.
26.0	34510.
26.8	36410.
28.0	38880.
30.2	43085.
32.3	47435.
33.7	49570.
34.8	52075.
37.4	56285.
39.0	58520.
40.5	60800.
42.5	63885.
44.1	66190.
45.8	68515.
49.0	72685.
50.5	74675.
52.0	76615.
53.5	78510.
54.9	80350.
56.0	81800.
57.5	83875.
60.0	87250.
61.3	89155.
62.4	90865.
63.8	92870.
66.6	96930.
67.4	98320.
68.6	100010.
69.5	101640.
70.8	103510.
73.7	107855.
75.3	110010.
78.8	115090.
80.4	117250.
81.9	119450.
83.4	121585.
84.4	122920.

Tab. 5 - Continued.

TEST LRIV-1		TEST LRIV-2		TEST LRIV-3	
FLIGHTS	α (mm)	FLIGHTS	α (mm)	FLIGHTS	α (mm)
0	14.3	0	14.45	0	14.30
20	14.8	100	15.25	100	15.75
80	15.55	200	15.80	200	16.25
140	15.75	320	16.35	300	16.50
200	16.30	400	16.95	400	16.90
300	16.8	500	17.25	500	17.05
400	17.3	600	17.90	600	17.45
500	17.45	710	18.35	700	17.80
600	18.05	900	18.85	800	18.25
700	18.40	1000	19.25	900	18.60
800	18.75	1100	19.50	1000	18.70
900	19.05	1200	19.90	1100	19.30
1000	19.65	1300	20.20	1200	19.65
1100	20.20	1400	20.80	1300	19.73
1200	20.55	1500	20.90	1400	20.0
1300	21.00	1600	21.60	1500	20.30
1400	21.5	1700	22.0	1600	20.75
1500	22.0	1800	22.10	1800	21.60
1600	22.65	1900	22.60	2000	22.50
1700	23.75	2000	23.10	2200	23.55
1800	23.85	2100	23.45	2400	23.85
1900	24.60	2200	24.45	2500	24.45
2000	25.50	2310	24.85	2600	25.05
2100	26.30	2400	25.35	2700	25.65
2200	27.35	2510	26.15	2800	26.40
2300	28.60	2600	26.75	2900	27.10
2400	30.00	2700	27.40	3000	27.80
2500	31.35	2800	28.25	3100	28.75
2600	33.55	2900	29.10	3200	29.75
2660	33.60	3000	30.10	3300	31.65
2720	36.20	3100	31.0	3400	32.20
2800	39.9	3200	32.60	3500	33.80
2830	41.35	3300	34.05	3600	35.35
2860	44.0	3400	36.15	3700	38.20
2900	44.65	3500	38.40	3800	41.10
2960	46.70	3600	42.15	3900	46.6
2980	51.35	3700	46.0	4000	53.05
3000	52.50	3800	53.5	4100	61.25
3030	55.10			4200	65.75
3050	58.85			4300	78.60
3100	59.45				
3130	60.50				
3160	63.65				
3200	67.05				

Tab. 6 - Results of the variable amplitude-stiffened panels tests.

TEST LRIV-4	
FLIGHTS	α (mm)
0	14.10
100	15.25
200	16.0
300	16.35
400	16.75
500	17.15
600	17.60
700	17.90
800	18.50
900	18.65
1000	18.80
1100	19.25
1200	19.70
1300	20.10
1400	20.50
1500	21.15
1600	21.20
1700	21.80
1800	22.30
1900	22.85
2000	23.50
2100	24.10
2200	24.55
2300	25.30
2400	26.00
2500	26.90
2600	27.70
2700	28.70
2800	29.95
2900	31.30
3000	33.30
3100	35.15
3200	38.35
3340	43.0
3400	49.40
3430	55.0
3500	55.65
3540	57.90
3600	62.85
3670	68.85
3700	69.60
	83.70

TEST LRIV-5	
FLIGHTS	α (mm)
0	14.50
100	15.70
200	16.70
300	17.20
400	17.65
500	18.05
600	18.60
700	18.95
800	19.45
910	20.0
1000	20.50
1100	21.05
1200	21.60
1300	22.10
1400	22.75
1500	23.40
1600	24.30
1740	25.40
1800	25.85
1900	26.85
2000	27.95
2100	29.05
2200	30.35
2300	31.45
2400	33.45
2500	35.30
2600	38.30
2700	41.50
2760	43.55
2800	46.40
2840	51.70
2900	53.05
2940	56.80
3000	61.95

TEST LRIV-6	
FLIGHTS	α (mm)
90	15.50
140	15.75
200	16.25
300	16.80
400	17.40
500	17.70
600	18.0
700	18.35
800	18.85
900	19.20
1000	19.60
1100	20.0
1200	20.40
1300	20.80
1400	21.25
1500	21.85
1600	22.40
1700	23.20
1800	23.85
1900	24.80
2000	25.65
2100	26.10
2200	27.10
2300	28.25
2400	29.50
2500	30.65
2600	32.70
2700	35.10
2800	38.65
2840	41.60
2900	42.30
3000	49.60
3060	56.40
3200	57.40
3160	60.20
3200	63.0
3300	67.40
3340	70.40
3400	74.50
3500	91.50

Tab. 6 - Continued.

TEST	σ_y	σ_R	K_c app
LAZ-01(A)	55.3	58.1	178.1
LAZ-02(A)	56.0	59.8	175.5
LAZ-03(A)	54.6	59.0	178.1
LAZ-04(A)	55.7	59.8	186.5
LAZ-05(B)	55.0	59.6	186.5
LAZ-07(B)	55.3	59.8	187.3
LAZ-08(A)	55.3	59.8	182.3
LAZ-09(B)	56.6	61.1	185.6
LRSV-7(B)	56.0	60.2	191.5
LRSV-9(B)	56.0	60.4	186.5
LRSV-10(B)	55.8	60.2	194.0
LRSV-11(A)	56.0	60.0	191.5

σ_y = yield stress (Kg/mm²)

σ_R = tensile strength (Kg/mm²)

K_c app = apparent K_c , calculated utilizing the maximum load and the crack initial half-length from experimental data (Kg/mm^{3/2}).

Tab.A.1 - Certain mechanical properties of a few flat panels utilized in the tests.

TEST N.	MATERIAL	PANEL TYPE	LOAD SPECTRUM	S _{MAX} (Kg/mm ²)	N° OF SPECIMENS
1	2024-T3	simple	C.ampli.	R=-1.÷.6	10
2	"	"	FALSTAFF	20.0	6
3	"	"	"	24.0	6
4	"	"	MINITWIST	7.0	6
5	"	"	"	10.0	6
6	"	"	GAUSSIAN RANDOM	to be def.	6
7	"	"	"	"	6
8	"	strip st. rivet A	C.ampli.	R= 0.4	6
9	"	strip st. rivet B	"	"	6
10	"	"	FALSTAFF	20.0	6
11	"	"	"	24.0	6
12	"	"	MINITWIST	7.0	6
13	"	"	"	10.0	6
14	"	"	GAUSSIAN RANDOM	to be def.	6
15	"	"	"	"	6
16	"	2 st. rivet B	FALSTAFF	20.0	6
17	"	"	"	24.0	6

Tab.A.2 - Program of tests for the third year's research.

END

DATE
FILMED

5 81

DTIC